THE ROLE OF THE TM2-HAMP JUNCTION IN CONTROL OF THE SIGNALING STATE OF THE ASPARTATE CHEMORECEPTOR OF *E. COLI*

A Dissertation

by

GUS ALAN WRIGHT

Submitted to the Office of Graduate Studies of
Texas A&M University
in partial fulfillment of the requirements for the degree of

DOCTOR OF PHILOSOPHY

August 2009

Major Subject: Biochemistry

THE ROLE OF THE TM2-HAMP JUNCTION IN CONTROL OF THE SIGNALING STATE OF THE ASPARTATE CHEMORECEPTOR OF *E. COLI*

A Dissertation

by

GUS ALAN WRIGHT

Submitted to the Office of Graduate Studies of
Texas A&M University
in partial fulfillment of the requirements for the degree of

DOCTOR OF PHILOSOPHY

Approved by:

Chair of Committee,	Michael D. Manson
Committee Members,	Donald W. Pettigrew
	Ryland Young
	Paul Cremer
Head of Department,	Gregory D. Reinhart

August 2009

Major Subject: Biochemistry

ABSTRACT

The Role of the TM2-HAMP Junction in Control of the Signaling State of the Aspartate Chemoreceptor of *E. coli*. (August 2009)

Gus Alan Wright, B.S, University of Alabama at Birmingham

Chair of Advisory Committee: Dr. Michael D. Manson

The mechanism of allosteric coupling between the external ligand-binding domain and the internal signaling domain of bacterial chemoreceptors is poorly understood. Genetic, biochemical, and biophysical evidence suggests that transmembrane helix 2 (TM2) undergoes a piston-like displacement of approximately 1-3 Ångstroms toward the cytoplasm upon the binding of aspartate to the Tar receptor. The signal is then transmitted to the cytoplasmic signaling domain via the HAMP domain, a conserved motif found in all methyl-accepting chemotaxis proteins (MCPs) and most histidine protein kinases (HPKs). HAMP forms a parallel four-helix bundle consisting of a dimer of two amphipathic helices (AS1 and AS2) connected by a flexible linker.

The MLLT sequence between residues Arg-214, at the end of TM2, and the conserved residue Pro-219, at the beginning of AS1 of the HAMP domain (the TM2-HAMP junction), is predicted to be able to form a helical extension of TM2. We hypothesized that perturbing the native secondary structure and/or the length of the TM2-HAMP junction would disrupt the ability of HAMP to communicate the input signal from TM2 to the kinase-control domain. To test this hypothesis, we designed two

experiments. First, constructs were made in which 1 to 3 Gly residues were inserted between T218 and P219. Second, Tar variants were constructed in which 1 to 9 Gly residues were inserted between R214 and P219. The results suggest that increasing the length and flexibility of the TM2-HAMP connection tends to uncouple signal propagation between the TM2 and the HAMP elements and suggests that HAMP alone causes an inhibitory effect on the cytoplasmic signaling domain.

To determine whether the predicted helical register of the MLLT sequence is an important component of the propagation of the transmembrane signal from TM2 to the HAMP domain, we added and subtracted helical residues to the MLLT sequence. The results suggest that helical register and length of the TM2-HAMP junction are essential for optimal receptor function.

DEDICATION

I dedicate this dissertation to my Mother and Father, Jack and Marilyn Wright, for their unwavering support and encouragement though my undergraduate and graduate studies. I also dedicate this dissertation in memory of my cousin, Michael Wright; grandmother, Edith Morgan; and great aunt, Mary Crisler.

ACKNOWLEDGEMENTS

I am extremely grateful for the opportunity to work with extremely talented colleagues during my graduate tenure. I am grateful to the members of the Manson lab, especially Drs. Roger Draheim, Brian Cantwell, and Run-Zhi Lai, for the many enlightening and intellectually stimulating discussions over many scientific ideas. I am also grateful for the excellent work environment and the camaraderie we all shared in the Manson lab. I am also grateful for the opportunity to work with very talented undergraduate students, especially Rachel Crowder. She was very instrumental in the progress I have made as a graduate student and a researcher.

I greatly appreciate the members of my doctoral advisory committee for their patience and willingness to advise and guide me through my graduate career. I am especially grateful for the opportunity to work and learn from my mentor and committee chair, Dr. Michael D. Manson. Without his patience, guidance, and support I would not be the scientific researcher I am today.

I would also acknowledge my family for their unwavering support, patience, and encouragement throughout my graduate career. I am also grateful for the opportunities my parents have given me to obtain higher education.

TABLE OF CONTENTS

LIST OF FIGURES

FIGURE Page

CHAPTER I

INTRODUCTION

Escherichia coli cells are motile and respond to a plethora of environmental stimuli

Escherichia coli is a gram-negative, rod-shaped enteric bacterium that is 2-4 μm long and 0.7 μm wide. Locomotion through liquid or semi-solid media is driven by the rotation of 4-8 peritrichous flagella. Counterclockwise rotation of the flagella results in the formation of a left-handed helical bundle of flagellar filaments (*1*). This bundle propels the cell forward in a "run," at speeds of up to 40μm/s. Clockwise rotation of the flagella results in the dissociation of the bundle and a rapid, random reorientation of the cell, called a "tumble" (*1*). In a homogeneous liquid environment, *E. coli* cells alternate between intervals of running of several seconds interspersed with shorter intervals of tumbling. This motion generates a three-dimensional "random walk" (*2*). Modulating the CW/CCW bias of the flagellar motors allows the cell to move toward favorable or away from unfavorable environmental conditions, respectively.

When a cell moves toward a favorable environment, tumbling (CW rotation) is suppressed. Since the reorientation of a tumbling cell in three dimensional space is random, the net movement up or down an attractant or repellant gradient is termed a "biased random walk" (*2*) (Figure 1).

E.coli cells move up an increasing gradient of attractant and down a decreasing gradient of repellent. This behavior is called chemotaxis. In *E.coli*, there are four

---

This dissertation follows the style of *Biochemistry*.

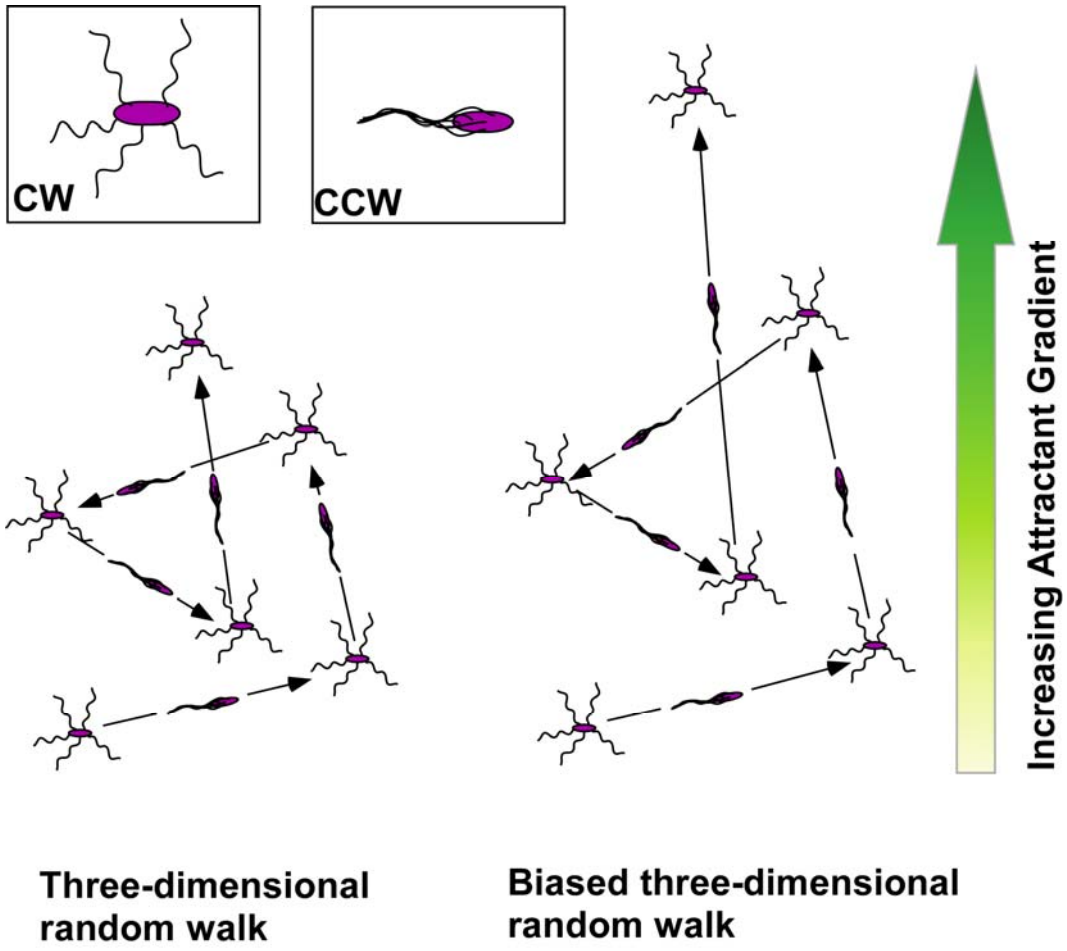

Figure 1. Chemotaxis of *E.coli* in a gradient of chemoeffector. Behavior of an *E. coli* cell in an isotropic environment (left) and in a gradient of attractant (right). In both cases the cell swims in a relatively straight line (runs), punctuated by transient and stochastically distributed three-dimensional reorientations (tumbles). The result is a three-dimensional random walk. In the presence of attractant, the cells suppress the probability of tumbling and thereby increase the time spent in a run as the cell moves toward higher concentrations of attractant. The cells exhibit a biased random walk as they migrate toward increasing concentrations of attractant.

transmembrane methyl-accepting chemotaxis proteins (MCPs): the serine receptor (Tsr), the aspartate/maltose receptor (Tar), the dipeptide/thymine receptor (Tap), and the ribose/galactose/glucose receptor (Trg) (*3-8*). Aer, which is not methylated, mediates redox chemotaxis (*9-11*). Aspartate and serine bind directly to Tar and Tsr, respectively. In contrast, maltose, ribose, galactose, glucose, and dipeptides first bind to their cognate periplasmic binding proteins, which then interact with the MCPs. L-leucine and indole are sensed as repellents by Tsr, whereas Ni^{2+} and a few other divalent cations are sensed as repellents by Tar (*5, 12, 13*).

E. coli chemoreceptors have a defined transmembrane architecture

Tar and Tsr exist as homodimers and have five distinct functional domains (*14*) (Figure 2). The periplasmic sensing domain is composed of a four-helix bundle (α1-4) that binds attractants at the dimer interface (*15-17*). The transmembrane region anchors the receptor to the membrane and serves as a conduit for the signal generated in the periplasm to traverse the membrane to the cytoplasm. Transmembrane region one (TM1) anchors the receptor in the membrane and stabilizes the homodimer (*18*). Transmembrane region two (TM2) is more dynamic, and it transfers the signal from the periplasm to the cytoplasm. The HAMP (Histidine kinase, Adenylate cyclase, Methyl – accepting chemotaxis proteins, Phosphatase) domain is a cytoplasmic extension of TM2 that is composed of two amphipathic helices (AS1 and AS2) connected by a 14-residue linker (*19, 20*). Adjacent to the HAMP domain is the cytoplasmic domain which consists

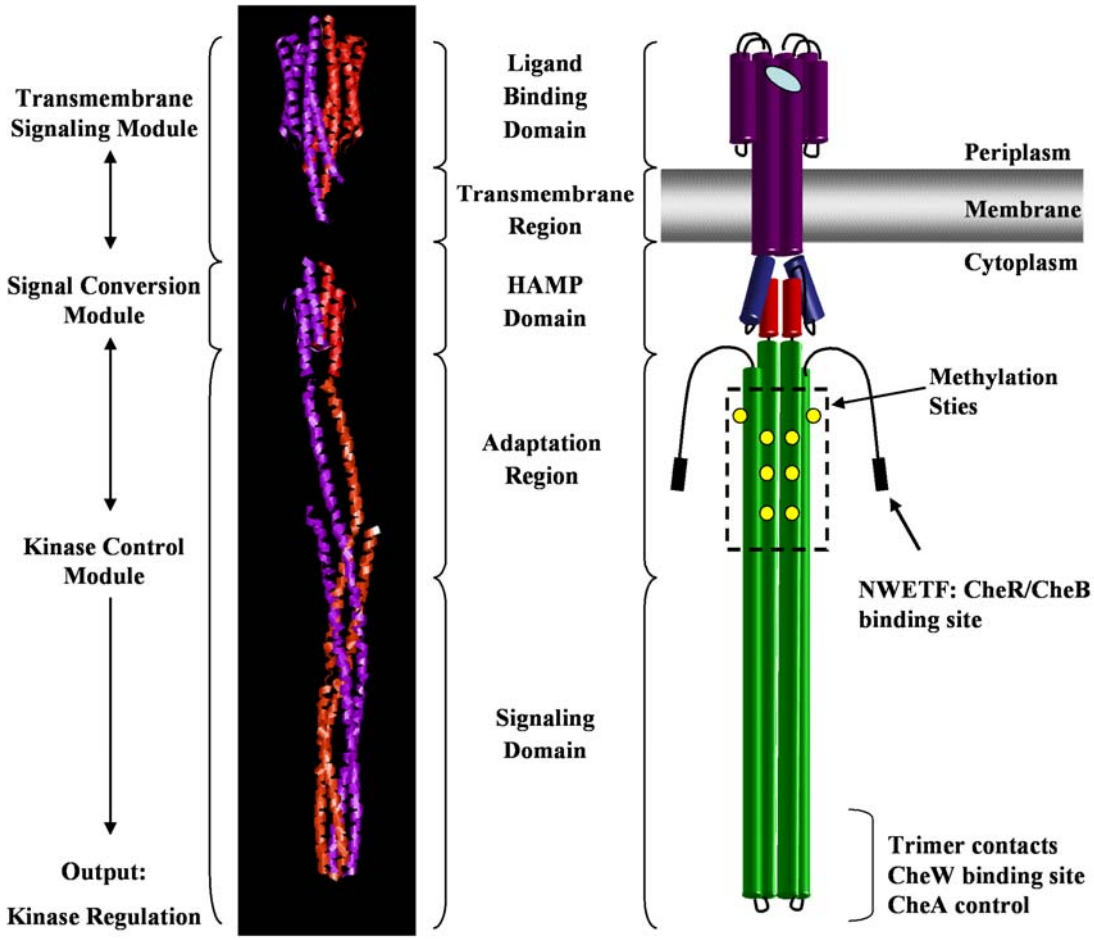

Figure 2. The chemoreceptor dimer. A ribbon structure (left) and a cartoon (right) depict the three-dimensional structure of a chemoreceptor homodimer. The modules of the receptor (transmembrane-signaling, signal-conversion, and kinase-control) are indicated on the far left. The functional domains/regions within the modules are indicated in the middle. The transmembrane region is composed of TM1 and TM2. The important functional features of the receptor are indicated at the right. The cytoplasmic domain is approximately 200Å in length.

of the adaptation and signaling domains. The cytoplasmic domain is an extended four-helix coiled coil composed of the CD1, CD2, CD1', and CD2' helices. The adaptation domain contains four glutamyl residues that are substrates for adaptive methylation. The highly conserved region at the distal tip of the four-helix bundle binds the CheW coupling protein and the CheA kinase (*21-24*). The extreme C-terminal tail of the receptor is flexible and ends in an NWETF sequence that binds the proteins that carry out adaptive methylation, CheR and CheB (*25*). The Tap and Trg chemoreceptors have the same structure, except that they lack the NWETF sequence (*25*). Therefore, Tsr or Tar must be expressed in the cell for Tap and Trg to mediate chemotaxis.

Chemoreceptors function in higher order oligomers. The receptor homodimers form trimers of dimers that are stable in the presence of CheA and CheW (*22, 26-31*). These trimers of dimers can be composed of different types of receptor homodimers (*27-29, 32*). In the presence of CheA and CheW, the trimers of dimers form clusters near the poles of the cell that contain at least some of all six of the soluble chemotaxis proteins (*33-37*). These higher-order arrays are proposed to be responsible for the approximately 35-fold amplification of an attractant response (*38*).

A phosphorelay controls flagellar rotation and receptor adaptation

The response regulators CheY and CheB are substrates for CheA. CheA transfers a phosphoryl group to Asp-57 on CheY, and CheY-P binds with high affinity to the FliM protein in the flagellar basal body (*39-44*). When FliM binds enough CheY-P there is a high probability of CW rotation (*45, 46*). The transition from CW to CCW rotation

requires less than a 1 μM change in intracellular CheY-P levels(*47*). When attractant binds to a chemoreceptor, the kinase activity of CheA is inhibited, thereby decreasing the intracellular levels of CheY-P. This results in a decreased occupancy of FliM by CheY-P and CCW rotation of the flagellum. Although CheY-P spontaneously dephosphorylates, the CheY-specific phophatase CheZ accelerates this process to ensure that CheY-P levels change rapidly in response to an attractant stimulus (*44, 48-50*)

Spatial chemical gradients are detected by a temporal mechanism that compares the current ligand occupancy to that of the ligand occupancy a few seconds earlier (*51*). This temporal comparison of the chemical gradient serves as a form of memory for the cells and is referred to as adaptation. Adaptation is mediated by the CheB methylesterase and the CheR methyltransferase, whose substrates are residues Glu 295, 302, 309, and 491. The glutamyl residues at positions 295 and 309 are originally translated as glutaminyl residues. CheR constitutively methylates these Glu residues (*52*), whereas phosphorylated CheB continually removes the methyl groups and deamidates the glutaminyl residues at positions 295 and 309 (*53, 54*). Once attractant binds the receptor, the CheB-P level decreases, which results in an overall net increase in receptor methylation that restores the ability of the ligand-bound receptor to stimulate CheA activity. This increase in methylation allows the cells to return to their normal run-tumble bias even though attractant is still present (*55, 56*). A schematic of the chemotaxis phosphorelay is depicted in Figure 3.

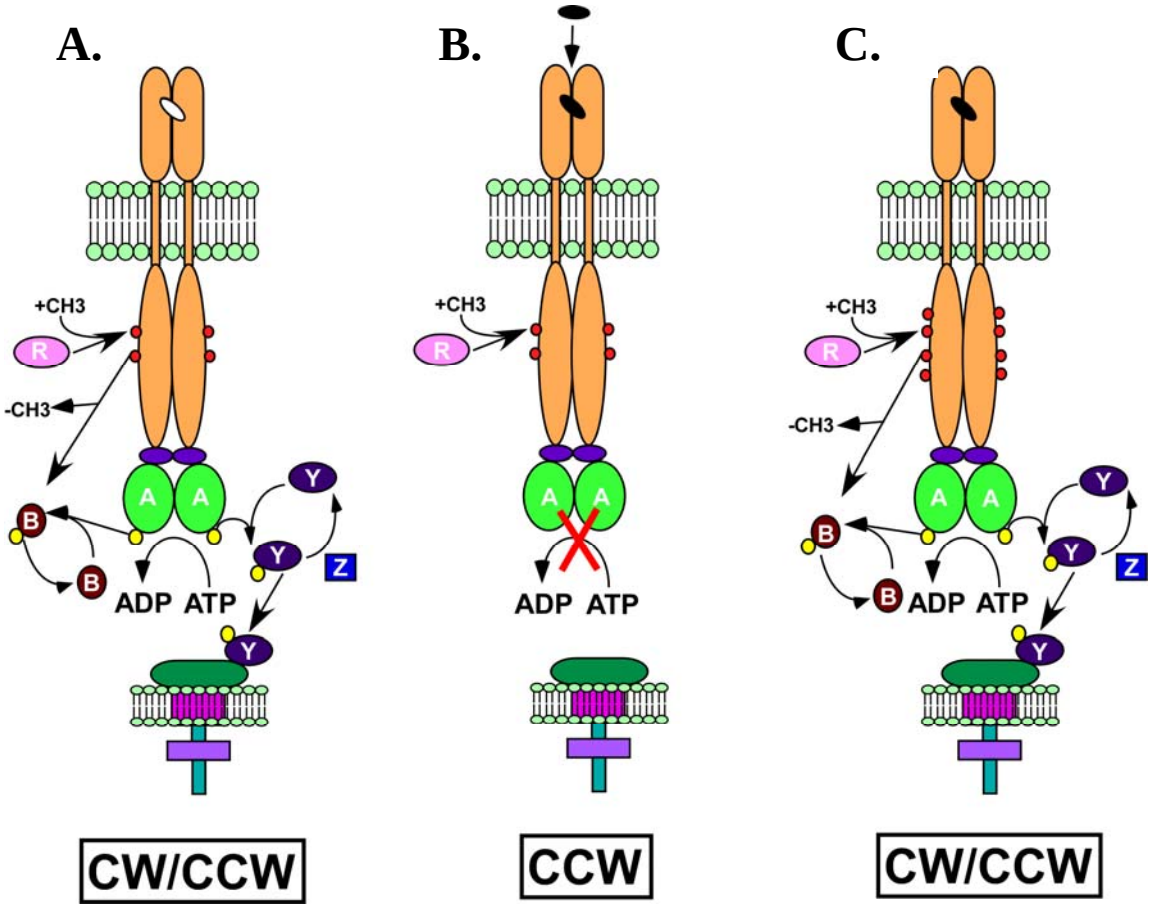

Figure 3. Chemotaxis signaling cascade. (A) Homodimeric chemoreceptors interact with the histidine kinase CheA through the coupling protein CheW to form a ternary complex. CheA autophosphorylation is stimulated by interaction with the ternary complex, and the phosphoryl group (yellow circle) is transferred to the response regulator CheY or the methylesterase CheB. The phosphorylated form of CheY (CheY-P) binds to the flagellar switch protein FliM, which causes CW rotation. The autodephosphorylation of CheY-P is accelerated by the CheZ phosphatase. The methyltransferase CheR constitutively adds methyl groups (red circles) to specific glutamyl residues on the receptor, whereas the phosphorylated form of CheB (CheB-P) demethylates the methyl glutamate residues. (B) Attractant (black oval) binds to the apical region of the periplasmic domain of the receptor and inhibits the CheA kinase at the distal cytoplasmic region of the receptor. The inhibition of the CheA kinase results in the decrease of the cellular concentrations of CheY-P and CheB-P. (C) The decrease of CheB-P upon addition of attractant, and the continuous methylation of the receptor by CheR, results in the increased methylation of the receptor. Methylation enhances the CheA stimulating ability of the receptor, thereby compensating for the effect of attractant binding on CheA activity.

Several structural modules regulate chemoreceptor kinase-stimulating activity

Several structural elements of the chemoreceptor modulate the activity of the CheA kinase. In Tsr, the isolated output domain interacts with CheA and CheW to generate the kinase-activating state of the receptor (*57, 58*). Receptors that cannot form trimers of dimers lack the ability to stimulate CheA, suggesting that isolated signaling domains are able to form dimers and trimers of dimers (*59, 60*). A truncated Tsr receptor containing HAMP and the output domain exhibits lower kinase activity than the output domain alone (J. S. Parkinson, personal communication), demonstrating that HAMP imposes a conformation on the output domain that inhibits kinase activity. The intact Tar and Tsr receptors activate CheA enough to elicit switching between CCW and CW flagellar rotation, suggesting that the periplasmic and TM domains suppress the inhibitory effect of HAMP on the output domain. Binding of attractant restores the ability of HAMP to inhibit the output domain, perhaps by functionally decoupling it from the periplasmic and TM domains. Schematic views of the proposed structural regulatory elements of chemoreceptors are depicted in Figure 4.

Transmembrane signaling relays allosteric input from periplasm to cytoplasm

One important question that remains in bacterial chemotaxis is the nature of the allosteric mechanism that couples the periplasmic ligand-binding domain of the receptor to the activity of CheA. In *E. coli* Tar, aspartate binds to one of two rotationally symmetric sites in the periplasmic domain, and the receptor exhibits extremely negative, half-of-sites cooperativity (*61*). This binding event also induces an approximately 20

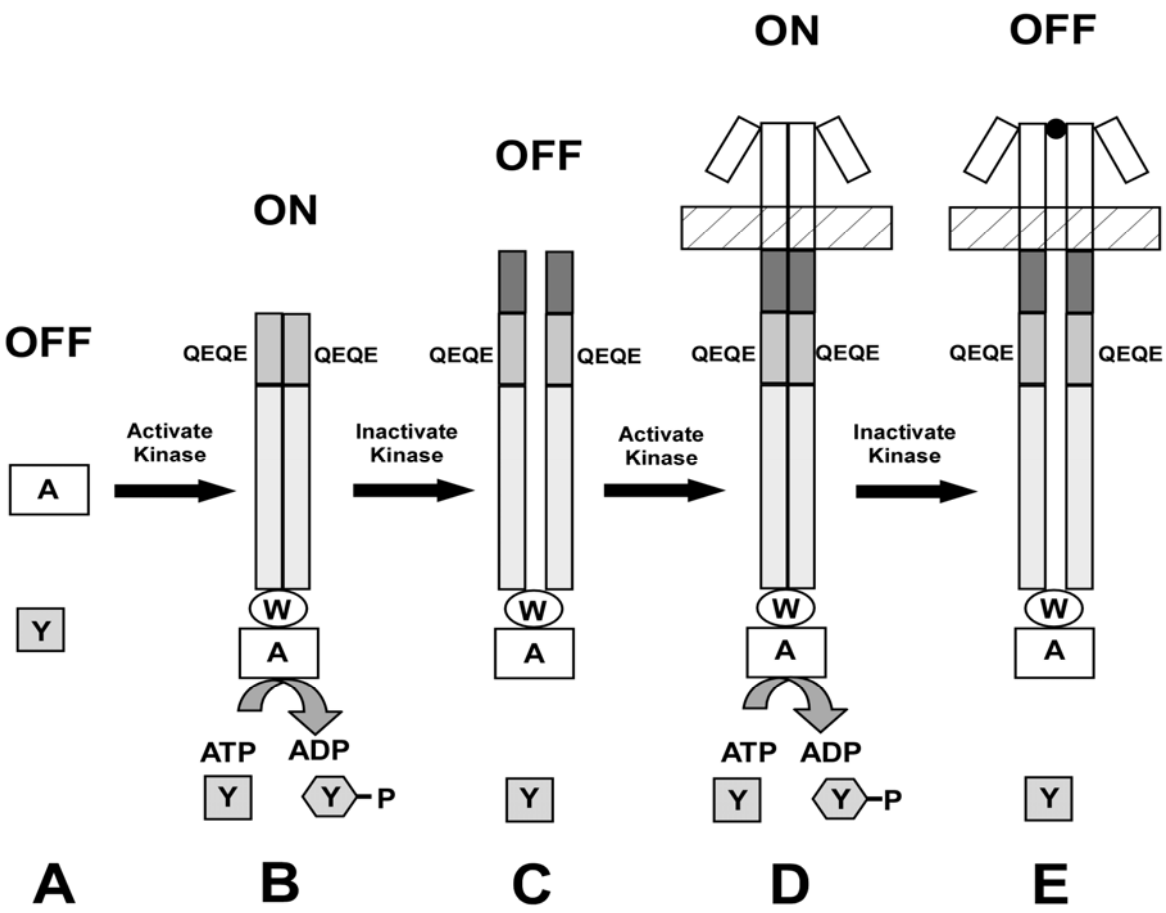

Figure 4. Illustration of the structural elements involved in chemoreceptor control of CheA kinase activity in the absence of CheRB. (A) In the absence of receptors, CheA activity is minimal. (B) In the presence of a receptor fragment containing the signaling domain (light gray rectangles) and CheW, CheA activity is increased several hundred fold, whether or not the adaptation domain (medium gray rectangles) is present. (C) The addition of HAMP (dark gray rectangles) to the adaptation and signaling domains presumably destabilizes the four-helix bundle of the signaling domain, resulting in a decrease in CheA activity. (D) In the absence of attractant, the periplasmic and TM regions in the intact receptor overcome the inhibitory effects of HAMP, resulting in a more-tightly packed four-helix bundle of the signaling domain, and therefore in CheA stimulation. (E) The addition of attractant (black circle) overcomes the inhibitory effects of the periplasmic and TM domains on HAMP, thereby restoring the inhibition of kinase activity by HAMP. Adaptive methylation restores the ability of receptors in panels C and E to stimulate kinase activity, presumably by allowing the helices of the signaling domain to pack more tightly.

degree rotation along the helical axes of the subunits (*62, 63*). Rotation of these helices breaks the rotational symmetry of the dimer. A small downward displacement of helix 4 is proposed to elicit signal propagation through TM2.

EPR and inter-TM disulfide crosslinking studies with Tar demonstrate that attractant binding causes a 1-3 Ångstrom piston-like displacement of TM2 toward the cytoplasm (*64, 65*). Similar experiments show that if TM2 is displaced toward the cytoplasm by crosslinking, the receptor is locked in the kinase-inhibiting state, whereas when TM2 is displaced toward the periplasm, the receptor is locked in a kinase-activating state (*66*). Similarly, methylation in response to attractant displaces TM2 toward the periplasm, returning it to the unstimulated position (*67*).

Using site-directed mutagenesis, Draheim et al. (*68*) modulated the signaling state of Tar by manipulating the positions of the (Trp209-Tyr210) aromatic anchor at the cytoplasmic end of TM2. As the tandem Trp-Tyr pair is moved toward the periplasm, TM2 is displaced toward the cytoplasm, causing the receptor to become increasingly biased toward the off state. If the tandem Trp-Tyr pair is moved toward the cytoplasm, TM2 is displaced toward the periplasm, resulting in receptors that are increasingly biased toward the on state. This experiment shows that the correct positioning of the aromatic anchor in the receptor is essential for normal CheA activation. Manipulating this position shifts the receptor toward the on or off states.

The adaptation region is considered to be the central processing unit (CPU) of the receptor (*69*). Mutations that neutralize acidic residues that reside on the cytosolic face of the CD1-CD2 four-helix bundle result in hyper-active receptors (*70*). Conversion of

four basic residues in the flexible C-terminal tail (Lys-523, Arg-528, Arg-540, and Arg-542) to Ala enhances CheA activity. However, replacing Arg-505 in CD2 with Ala and Asp residues reduces and abolishes Tar activity, respectively (*71*), suggesting that the CPU controls the packing of the CD1-CD2 four-helix bundle.

The HAMP domain plays a crucial role in transmembrane signaling

HAMP appears to play a significant role in transmitting ligand-induced conformational changes between the input (periplasmic and TM2) domains and the output (adaptation and signaling) domains. The HAMP domain is a 50-residue domain whose general properties are conserved in many transmembrane-signaling proteins in bacteria and archae (*72, 73*). HAMP domains are typically located between input and output domains in these signaling proteins. Chimeric proteins fusing heterologous input and output domains—including Taz (*74*), Trz (*75*), and NarX-Tar (*76*)—retain signaling properties. Results from these chimeras suggest that the mechanism of HAMP signaling is conserved among signaling proteins, although details of this mechanism continue to remain elusive.

Currently, a high resolution structure for a MCP HAMP domain does not exist. However, structural data obtained through an *in vitro* crosslinking experiment demonstrated that the MCP HAMP domain is composed of two amphipathic helices (AS1 and AS2) tethered by a flexible connector region (*77*). Recently, an NMR solution structure of the dimeric Af1503 HAMP domain from the thermophilic archeon *Archaeoglobus fulgidis* (*78*) revealed that AS1 and AS2 interact to form a parallel four-

helix bundle. AS1 and AS2 associate in an unusual knob-on-knob packing arrangement in which large hydrophobic residues come into contact with one another at the helix interface (Figure 5). Intersubunit disulfide crosslinking between AS1 and AS2 reveals that the Tar HAMP domain closely resembles that of the Af1503 structure (*79*). Additionally, mutational analysis of the AS1/AS2 connector region in Tsr also suggests that the structure of Tsr HAMP is similar to that of the Af1503 HAMP structure (*80*).

Two models exist to explain the effect of conformational changes in HAMP on transmembrane signaling (Figure 6). The first model, proposed by Williams and Stewart (*73*), suggests that, in one signaling state, AS1 and AS1' of the receptor dimer lie roughly parallel to and embedded in the cytoplasmic face of the cell membrane. In the other signaling state, AS1 and AS1' are displaced from the membrane, allowing them to interact with the hydrophobic face of AS2' and AS2 to form the four-helix HAMP bundle.

The second model suggests that AS1 and AS2 are always in a four-helix bundle and rotate relative to one another. The knob-on-knob packing arrangement of the HAMP domain can, via a 26-degree rotation of the AS1 and AS2 helices relative to each other, be converted into a knob-in-hole packing arrangement, in which large aliphatic residues of one helix fit into holes (corresponding to small residues) in adjacent helices. The knob-in-hole conformation may correspond to one signaling state, and the knob-on-knob conformation may correspond to the other. Neither conformation has been assigned to the "on" or "off" state, although the knob-on-knob packing is predicted to correspond to the "on" state (J. S. Parkinson, personal communication).

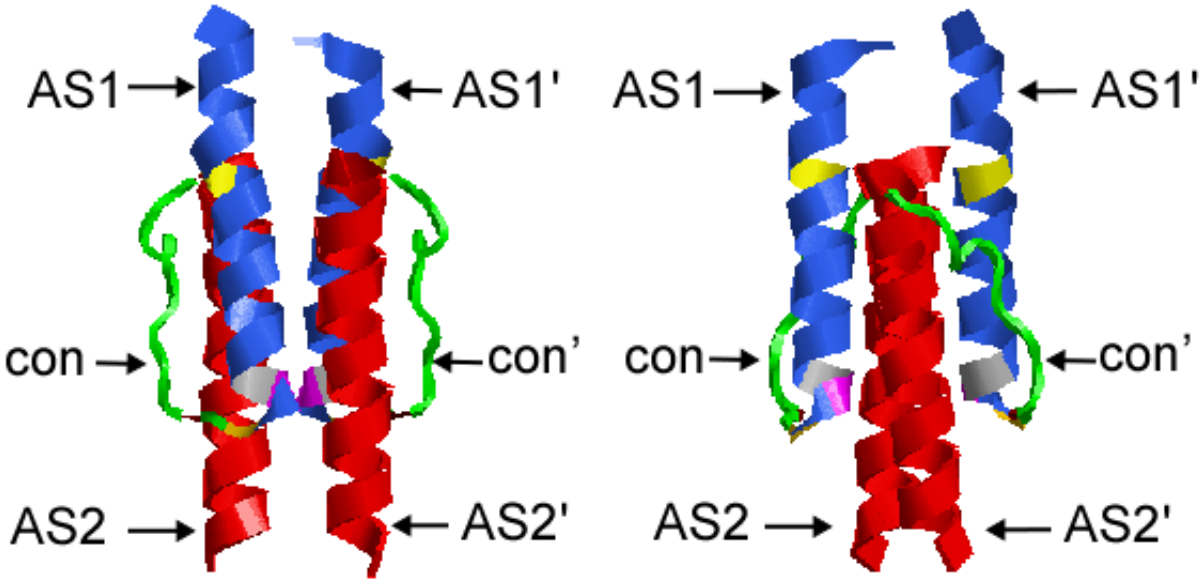

Figure 5. The four-helix bundle of the HAMP domain. The structure is based on the solution NMR structure of the Af1503 HAMP domain (*78*). The structure is a parallel four-helix bundle with an unusual knob-on-knob packing arrangement. AS1 and AS1' are labeled in blue, AS2 and AS2' are labeled in red, and the connector regions are labeled in green. Three residues in AS1 are labeled: Pro-283 (yellow), Ile-294 (grey), and Ala-295 (magenta). Pro-283 corresponds to Pro-219 in Tar; Ile-294 corresponds to Ile-230 in Tar; and Ala-295 corresponds to Ala-231 in Tar. These three residues are highly conserved in all MCPs, and the Pro residue is also conserved in most sensor histidine kinases (SHKs).

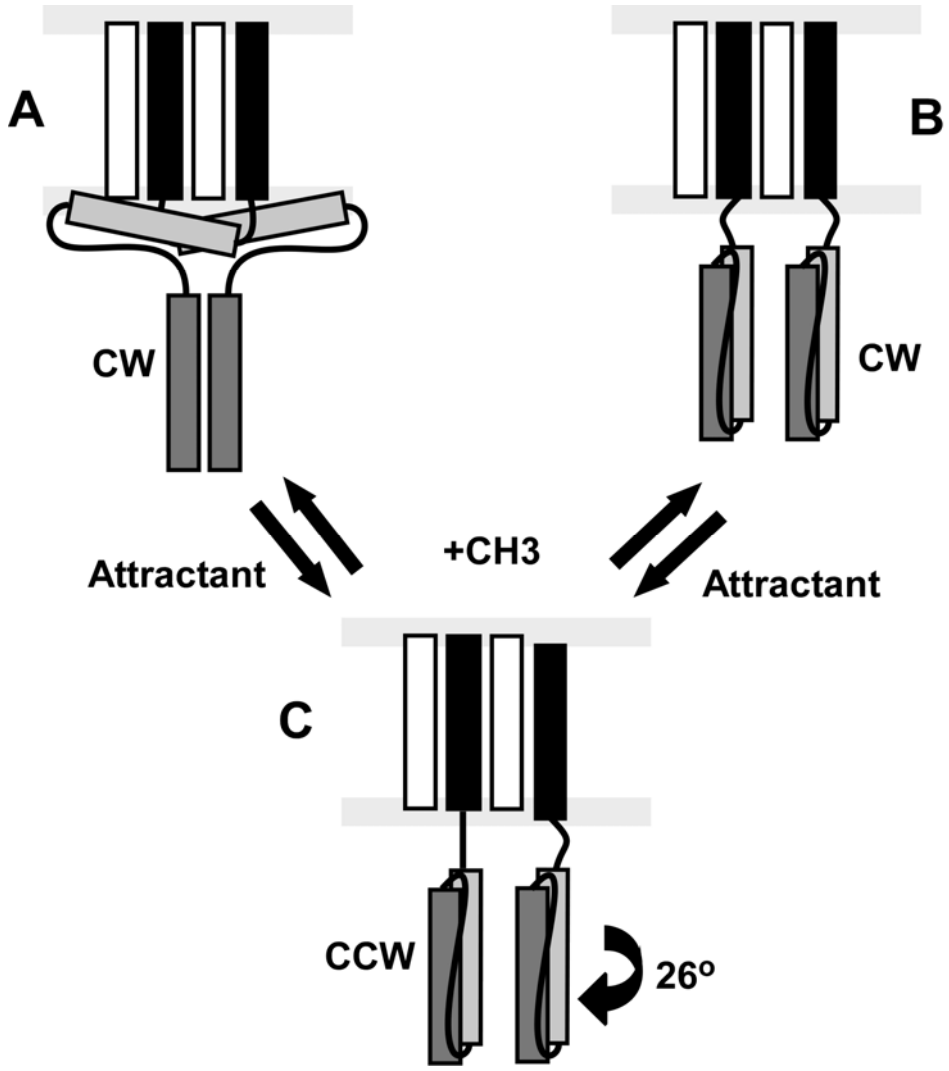

Figure 6. Two proposed models for HAMP signaling. (A) The membrane-association model proposes that AS1 and AS1' (light gray rectangles) reside within the cytoplasmic face of the inner membrane, whereas AS2 and AS2' (dark gray rectangles) form a dimer in the absence of ligand. Upon ligand binding, TM2 (black rectangles) is displaced toward the cytoplasm relative to TM1 (open rectangle), releasing AS1 and AS1' from the membrane and allowing AS2 and AS2' to interact with AS1' and AS1 in a parallel four-helix bundle. (B) The rotation model suggests that AS1-AS2' and AS1'-AS2 interact in a parallel four-helix bundle in the attractant-bound and unbound states. However, upon ligand binding, the helices undergo a 26^{o} rotation relative to one another. (C) The attractant-bound state is the same for both models of HAMP function. Adaptive methylation of CD1 and CD2 returns the HAMP to its prestimulated state.

The rotation model receives support from disulfide-crosslinking studies between AS1-AS2' and AS1'-AS2 in the intact Tar receptor (*79*). Crosslinking between AS1-AS2' and AS1'-AS2 results in receptors that are locked in kinase-activating or kinase-inhibiting states. The rotation model is especially attractive for receptors such as Aer, in which signals are generated through interaction of the HAMP domain with a cytoplasmic, FAD-binding PAS domain (*81, 82*).

Mutational analysis of the 14-residue connector region between AS1 and AS2 of Tsr HAMP suggests that relatively small conformational changes can shift the signaling states of the receptor (*80*). Amino acid substitutions at three residues within the connector (G235, L237, and I241) drastically affect receptor function. Replacements at L237 resulted in lock-on and lock-off outputs suggesting that this residue is important in the transition rate between signaling states. Mutations at I241 lock or bias the receptor toward the on-state. I241 packing thus seems to stabilize the off-state of the receptor. Presumably, substitutions at G235 disrupt the turn at the end of AS1 that is essential for the parallel helix packing.

Dissertation overview

The research presented in this dissertation investigates the importance of the MLLT residues between Arg-214 of TM2 and Pro-219 of AS1 (TM2-HAMP connector) on the ability of HAMP to communicate the input signal from TM2 to the kinase-control domain. In Chapter II we used two experiments to examine the effects of perturbing the secondary structure and length of the TM2-HAMP connector on the ability of HAMP to

communicate the signal from TM2 to the kinase control domain. First, Tar mutant constructs were made with 1, 2, and 3 Gly residues inserted between residues Thr-218 and Pro-219 in AS1 (TnG mutants). Second, Tar variants were made replacing the native sequence of the TM2-HAMP connector (MLLT) with 1 to 9 Gly residues (nG mutants). The majority of the Gly mutants were deficient in aspartate chemotaxis with the exception of the 4G mutant, which exhibited 80% of wild type chemotaxis. The majority were also CCW biased in a *cheR*$^+$*B*$^+$ strain, CCW-locked in a Δ*cheRB* strain, and over methylated in a *cheR*$^+$*B*$^+$ strain. In the TnG mutants there were no phenotypic differences between adding one Gly residue versus adding two and three Gly residues. Whereas in the nG mutants the receptors became increasingly deficient in signaling and chemotaxis as residues were added or subtracted from the 4G mutant. The results suggest that the addition of the Gly residues between TM2 and HAMP uncouples the communication between the two domains. However, methylation seems to compensate for the uncoupling of TM2 from HAMP and restores some aspartate chemotaxis and receptor activity. It also seems inconsistent with the idea that a rotation of TM2 within the membrane is propagated directly to HAMP. Thus, the simplest model to explain the mechanism of transmembrane signaling via direct rotational coupling of TM2 and AS1 via rotation about a continuous helical axis seems unlikely to be correct. The results from the nG mutants suggest that there is an optimal length for the TM2-HAMP connector – four residues.

In Chapter III we consider different modifications of this region in which residues were added or deleted from the MLLT sequence in the TM2-HAMP connector

(LLT mutants) that would be expected to retain the helicity of this region. This effort was undertaken to determine whether the predicted helical register of the MLLT sequence is an important component of the propagation of the transmembrane signal from TM2 to the HAMP domain. Most of the LLT mutants were deficient in aspartate chemotaxis with exception to the -1 mutant which exhibited approximately 60% of wild type chemotaxis. The majority of the LLT mutants also exhibited a CCW biased phenotype in a *cheR*$^+$*B*$^+$ strain, and were CCW locked in a Δ*cheRB* with the exception of a few mutants. These mutants were also overmethylated in a *cheR*$^+$*B*$^+$ strain with the exception of the -2 mutant which was demethylated. These results suggest that changing the helical register of the TM2-HAMP connection has profound effects on Tar function. Receptors in which the connector has roughly the same helical register as it does with the wild-type MLLT sequence are, as a rule, more active than receptors in which the helical register is altered. It appears that both the length and the proper helical register are important for optimal receptor function.

In Chapter IV, I discuss the implications of the mutations affecting the TM2-HAMP junction for our understanding of the control of CheA kinase activity and methylation-dependent adaptation. I also discuss why some proposed mechanisms for communication between TM2 and HAMP cannot be correct and suggest new experiments to test the other models.

CHAPTER II

THE EFFECT OF INSERTION OF VARIABLE NUMBERS OF GLY RESIDUES AT THE TM2-HAMP JUNCTION

Introduction

E. coli chemoreceptors are homodimers that consist of three control modules: 1) a transmembrane-sensing module; 2) a signal-conversion module; and 3) a kinase-control module. The transmembrane-sensing module contains the periplasmic ligand-binding domain, to which each monomeric subunit contributes a four-helix bundle, and transmembrane helices 1 and 2 (TM1 and TM2). The signal-conversion module is the HAMP (histidine kinase, adenylate cyclase, methyl-accepting chemotaxis protein, and phosphatase) domain, which is predicted to assume a dimeric, parallel four-helix bundle in at least one of its possible conformations. The cytoplasmic kinase-control module is an extended dimeric four-helix bundle that contains 36 heptad repeats in each monomer, 18 in the descending CD1 helix and 18 in the ascending CD2 helix. In its membrane-proximal portion, the CD1-CD2 bundle contains heptads with the four glutamyl residues in each subunit that are substrates for adaptive methylation and demethylation by CheR and CheB. The adaptation domain is joined, via a flexible glycine hinge, to a distal region that terminates with a distal hairpin loop. The heptads flanking the hairpin loop interact with CheA and CheW and comprise the signaling domain.

In the ligand-binding domain, aspartate binds to one of two rotationally symmetric sites in the periplasmic domain (*61*). Aspartate binding causes a symmetry-

breaking 20^{o} rotation along the helical axes of the domain (*62, 63*). It also causes a ~1-3 Ångstrom axial displacement of helix 4 of one subunit towards the cytoplasm (*65, 66, 68, 83-87*). This asymmetric signal is transmitted via TM2 to the adjoining HAMP domain, in which it is converted into a symmetric signal. From this point on, the signal is thought to be propagated as a rotation of the CD1-CD2 four-helix bundle that loosens the helical packing of the signaling domain to inhibit stimulation of CheA kinase activity.

The methylation sites within the adaptation domain are proposed to act as an electrostatic switch between the kinase-activating (on) and kinase-inhibiting (off) signaling states (*70, 88*). The aspartate-induced conformational change that destabilizes the signaling domain also increases the rate of methylation of the adaptation domain. Furthermore, the decreased kinase activity leads to a net dephosphorylation of CheB, which in turn decreases the methylesterase activity that demethylates the receptor. Increased methylation counteracts the attractant-induced destabilization of the four-helix bundle by neutralizing the electrostatic repulsion of the glutamyl residues in the adaptation domain. The result is that the kinase-control domain returns to its pre-stimulus conformation and resumes activation of CheA kinase to return the system to its original signaling state.

The MLLT sequence between residues Arg-214, at the end of TM2, and the conserved residue Pro-219, at the beginning of AS1 of the HAMP domain (the TM2-HAMP junction), is predicted to be able to form a helical extension of TM2 (*77, 78*). We hypothesized that perturbing the native secondary structure and/or the length of the

TM2-HAMP junction would disrupt the ability of HAMP to communicate the input signal from TM2 to the kinase-control domain. To test this hypothesis, we designed two experiments. First, constructs were made in which 1 to 3 Gly residues were inserted between T218 and P219. Second, Tar variants were constructed in which 1 to 9 Gly residues were inserted between R214 and P219.

The capacity of each protein to support aspartate and maltose chemotaxis in a *cheR*$^+$*B*$^+$ strain was measured. The intrinsic signaling properties of all of these Tar proteins expressed as the sole chemoreceptor in cells with and without the adaptive methylation system (i.e., in *cheR*$^+$*B*$^+$ and Δ*cheRB* strains) were also examined. Finally, the baseline (unstimulated) methylation state and the methylation states after addition of aspartate (attractant) and Ni^{2+} (repellent) were determined for each protein. The results indicate that increasing the length and flexibility of the TM2-HAMP connection essentially decouples the transmembrane-sensing and HAMP domains. However, the significant residual function of some of these proteins also suggests that a continuous helical connection between TM2 and HAMP is not essential for either transmembrane signaling or for maintaining a nearly normal baseline CheA kinase-stimulating activity.

Materials and methods

Bacterial strains and plasmids. Strains RP3098 (Δ(*flhD-flhB)4*) and VB13 (*thr*$^+$ *eda*$^+$ Δ*tsr7201 trg::*Tn*10* Δ*tar-tap5201*) are derived from the *E. coli* K-12 strain RP437. Strain HCB436 is a Δ*cheRcheB* derivative of VB13. Plasmid pMK113, a derivative of pBR322, was utilized to express the mutated *tar* gene at near-physiological

concentrations. Plasmid pBAD18 was used to over-express *tar* with an additional C-terminus seven-residue linker (GGSSAAG) and V5 epitope attached to the 3' end of *tar.* Mutations were introduced into the *tar* gene via standard site-directed mutagenesis (Stratagene).

Measuring chemotaxis to attractants. Swarm assays were conducted to measure chemotaxis toward attractants carried out by VB13 cells expressing the various Tar variant proteins expressed from plasmid pMK113. Semi-solid motility media agar plates were made with the addition of 3.25 g/L BD Bactoagar, Che salts (10 mM potassium phosphate (pH 7.0), 1 mM $(NH_4)_2SO_4$, 1 mM Mg SO_4, 1mM glycerol), 1 mM $MgCl_2$, 90 mM NaCl, 0.1 mM attractant (aspartate and maltose, separately), 0.2% THML, 0.1% B1 vitamin, and 100 μg/mL ampicillin. Plates were stabbed with isolated colonies and incubated at 30ºC. First measurements (ring diameter in millimeters) were taken after 8 h. Subsequent measurements were taken every 4 h until colonies had swarmed for a full 24 h. The rate of chemotactic-ring expansion was measured as mm/hour and is expressed as a percentage of the wild-type rate on the same plate.

Observation of tethered cells. VB13 and HCB436 cells harboring the various Tar variant proteins expressed from plasmid pMK113 were grown overnight in tryptone broth (TB) with the addition of 50 μg/mL ampicillin (Amp50) at 30°C. Overnight cultures were then back-diluted 1:100 in TB-Amp50 and grown at 30°C with agitation until a culture OD_{600} of ~0.6. Cells were then harvested by centrifugation and resuspended in tethering buffer, containing 10 mM potassium phosphate, pH 7.0, 0.1 M NaCl, 0.01 mM EDTA, 0.02 mM L-methionine, and 20 mM sodium lactate.

Chloramphenicol was added at 20 μg/mL chloramphenicol to prevent regrowth of flagellar filaments after shearing. Cells were sheared in a Waring blender with 8 repetitions of 7 second intervals of shearing with 13 second pauses. Cells were collected by centrifugation, washed 3 times, and finally resuspended in tethering buffer with chloramphenicol. A 20 μL aliquot of a 200-fold dilution of anti-flagellar filament antiserum was added to 20 μL of these cells. Round glass coverslips of 12 mm diameter were soaked in fuming nitric acid for 1 hour. Apiezon-L grease was added carefully around the edge of these cover slips using a syringe, and 40 μL of the cell/antibody mix was added to the center of the cover slip.

The coverslips were incubated in a humidity chamber constructed by placing a ring of wet paper toweling around a piece of dry filter paper in a Petri dish. Cover slips were placed facing upward into the humidity chamber for 30 min at 30ºC. After incubation, cover slips were affixed to a flow chamber (*89*), and non-tethered cells were washed from the solution. Cells were observed under phase contrast at 1000x magnification using the 100x oil immersion objective and 10x eyepiece of an Olympus BH-2 microscope. Rotating cells were videotaped, and 100 individual cells were observed during a 30 sec playback to determine their rotational bias and switching frequency.

In vivo *methylation.* VB13 cells containing plasmid pMK113 expressing the different V5-tagged Tar variants were grown overnight in tryptone broth (10 g/L tryptone, 8 g/L NaCl) containing 50μg/ml ampicillin at 30ºC. Overnight cultures were back-diluted 1:100 into the same medium and shaken at 30ºC for another 5.5 hours until

an OD_{600} of ~0.6 was reached. Cells were harvested by centrifugation, washed three times with 10 ml of 10 mM potassium phosphate buffer (pH 7.0) containing 0.1mM EDTA, and then resuspended in 5 ml of 10 mM potassium phosphate (pH 7.0), 0.1 mM EDTA, 10 mM sodium DL-lactate, and 200 µg/ml of chloramphenicol. One ml aliquots were placed into 10 ml scintillation vials and incubated for 10 min at 30ºC with shaking. The cells were then incubated for another 30 min after adding L-methionine to a final concentration of 0.01 mM. Buffer containing L-aspartate at 100 mM or $NiSO_4$ at 10 mM, or an equal volume of buffer alone, was added to the cells, and they were incubated for another 20 min at 30^{o}C. Reactions were terminated by addition of 100 µl of 100% TCA and incubated on ice for 15 min. Denatured proteins were pelleted and subsequently washed with 1% TCA and acetone. The dried pellet was resuspended into 100 µl of 2X SDS loading buffer.

The resuspended pellets were subjected to 3 freeze/boil cycles, each lasting 10 min in order to denature proteins. A 20 µl aliquot of each sample was loaded into a 7.5% SDS-PAGE gel. Current was applied to the gel in order to separate proteins based on apparent molecular weight. Once electrophoresis was complete, protein from the gels was transferred to nitrocellulose paper. A Western blot was performed by adding anti-V5 epitope antibody (Invitrogen) to the nitrocellulose paper. Visualization of protein was achieved using goat-anti-mouse antibody conjugated to an alkaline phosphatase (Bio-Rad).

Standards were run with a mixture of Tar proteins containing equal proportions of the V5-tagged versions of the EEEE, QEQE, and QQQQ forms of the receptor. The

glutaminyl residues have the same effect on protein migration as methylated glutamyl residues(*90*) , so that the standard serves as an estimate of the extent of methylation of Tar in the samples. Each charge neutralization, whether by methylation or amidation, increases the migration rate of the corresponding protein by a detectable amount.

Results

Inserting a flexible Gly linker between Thr-218 and Pro-219 of AS1 in Tar. We examined the effect of inserting one, two, and three Gly residues (T1G, T2G, and T3G) between Thr-218 and Pro-219. In these constructs, the MLLT helical extension of TM2 remains intact (Figure 7). In particular, the Leu-216 equivalent in Tsr, which has been shown to be particularly critical for normal signaling by the closely related Tsr chemoreceptor of *E. coli* (J. S. Parkinson unpublished results) is retained.

The ability of the Tar TnG proteins to mediate chemotaxis. Each of the TnG mutants was tested for its ability to perform aspartate taxis in semi-solid minimal agar when expressed in strain VB13. The rate of ring expansion supported by wild-type and each mutant Tar expressed at near-physiological levels was measured. The T1G mutant supported 50% of the chemotaxis-ring expansion rate seen with wild-type Tar (Figure 8). The T2G and T3G were slightly worse, supporting 40% of the expansion rate observed with wild-type Tar. Maltose chemotaxis and aerotaxis exhibited the same trends as the aspartate taxis. However, all of these proteins did support some level of chemotactic ring formation and expansion. Tellingly, the chemotactic rings on aspartate plates were sharper, indicating that cells expressing the mutant proteins might accumulate more

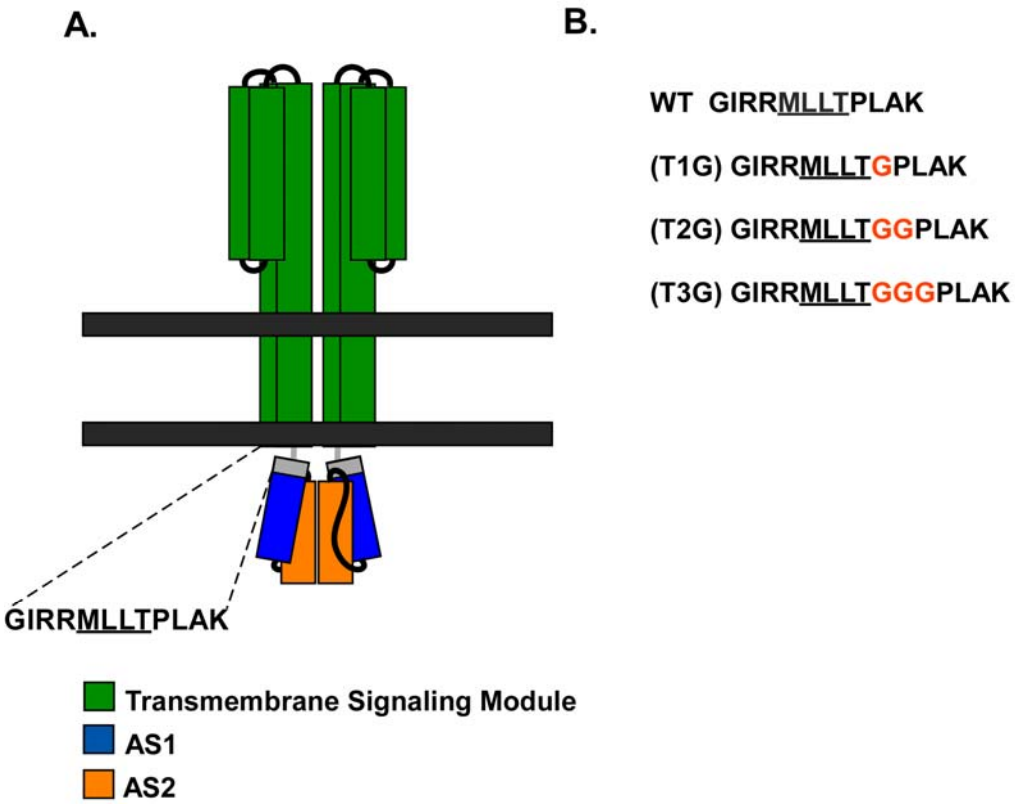

Figure 7. Insertion of multiple Gly residues between Thr-218 and Pro-219. (A) A cartoon of the transmembrane-signaling module (green rectangles), which is connected to AS1 (blue rectangles) and AS2 (orange rectangles) through the TM2-HAMP junction (gray rectangles). The transmembrane-signaling module contains the periplasmic ligand-binding domain and transmembrane helices 1 (TM1) and 2 (TM2), which traverse the membrane. AS1 is predicted to be a helical extension of TM2 that is connected to AS2 through a flexible connector. (B) The wild-type sequence of the C-terminal end of TM2, the TM2-HAMP junction, and the N-terminus of AS1. The TnG mutants are shown below the wild-type sequence. Inserted Gly residues are colored red.

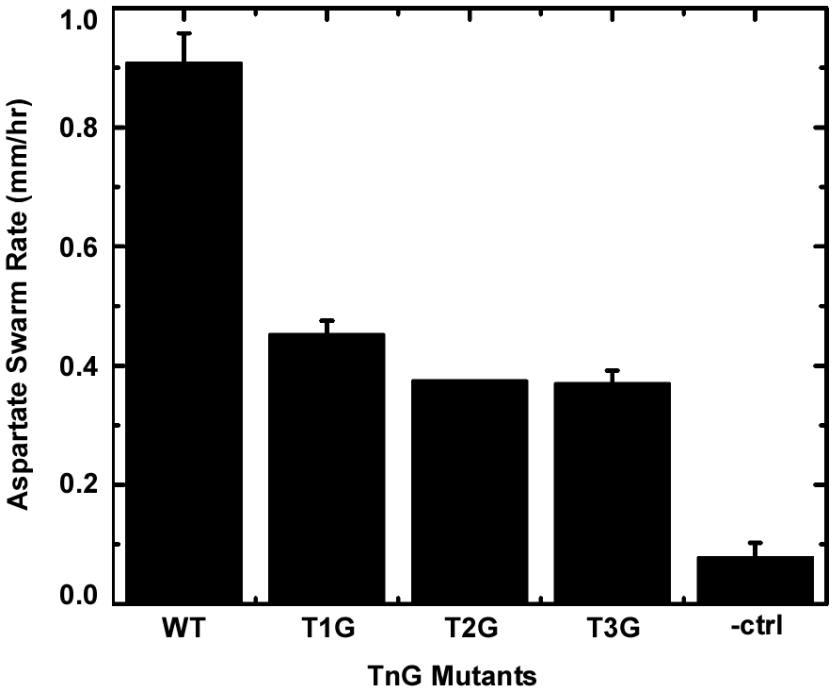

Figure 8. The aspartate chemotaxis-ring expansion rates of cells expressing the TnG mutant receptors. The rate at which the chemotaxis-ring diameter increased, measured in mm/h, was measured in VB13 (*cheR*$^+$*B*$^+$) cells expressing wild-type or mutant receptors from pMK113CV5. The error bars represent the standard deviation of the mean, with n=3.

strongly in regions in which the aspartate gradient is particularly steep. The inescapable conclusion, however, is that TM2 and the kinase-control domain are not completely uncoupled in these proteins.

Rotational biases and mean reversal frequencies of TnG Tar-expressing cells. VB13 cells expressing the T1G, T2G, and T3G mutants from plasmid pMK113 were more CCW biased than VB13 cells expressing wild-type Tar. Of 99 cells expressing wild-type Tar, 63 had approximately equal distributions of CCW to CW rotation, 33 cells were CCW biased, and 3 were CCW locked (Figure 9A). The wild-type mean reversal frequencies (MRF values) were also somewhat lower, being 0.672 for cells expressing wild-type Tar, 0.45 reversals/sec for T1G, and 0.42 reversals/sec for T2G and T3G (Figure 10). Notably, little if any difference in either the bias or MRF values was seen among the three TnG variants, suggesting that the effect of inserting only one Gly residue at this position imposes almost the full effect seen with insertions at this point.

Adaptive methylation of the TnG proteins in vivo. The methylation state of the various V5-tagged receptors was measured in VB13 cells. Previous work (*90*) has shown that these proteins function essentially as their untagged variants. In the absence of ligand, the wild-type receptor was primarily in the unmethylated state. Addition of 10 mM $NiSO_4$ further decreased methylation, resulting in a totally unmethylated receptor. With addition of 100mM aspartate, the wild-type receptor is primarily in the fully methylated state. All of the TnG receptors were overmethylated, although they still showed additional methylation after the addition of aspartate and decreased methylation after the

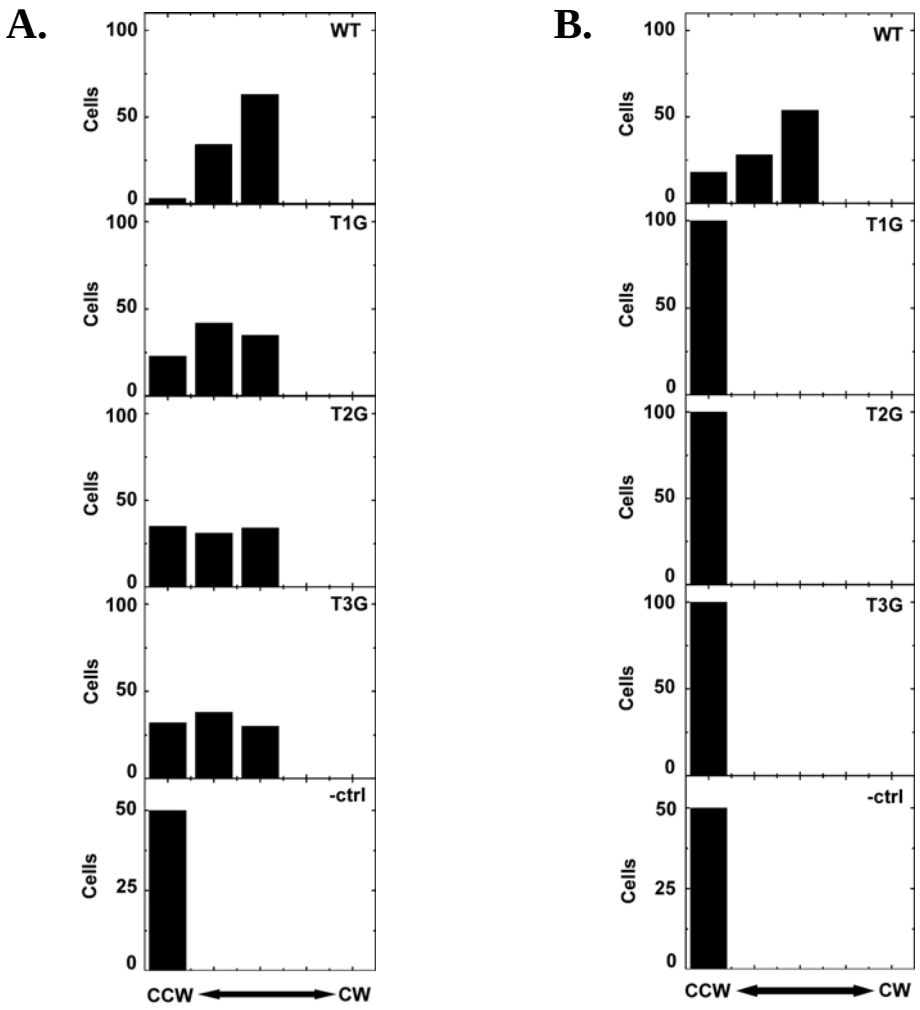

Figure 9. Rotational biases of flagella of tethered cells expressing the TnG mutant receptors in strains with and without the adaptive methylation machinery. (A) Transducer-depleted, methylation-competent cells (VB13) expressing wild-type or TnG mutant receptors were tethered, and their flagellar rotation was monitored over a 30 sec interval. The cells were placed into one of five categories based on their CW/CCW rotational biases: CCW locked, CCW biased, CCW/CW, CW biased, and CCW locked (graphically depicted above from left to right). One hundred cells were measured for each strain. (B) The rotation of tethered cells lacking the adaptive methylation machinery (HCB436) and expressing wild-type or TnG mutant receptors was monitored over a 30 sec interval. The cells were put into one of five categories, as described above. One hundred cells were measured for each strain.

addition of Ni^{2+} (Figure 11). Thus, these receptors can partially compensate for their intrinsic CCW bias by increasing their level of methylation.

Signaling defects of the TnG mutants are exaggerated in the absence of the adaptation machinery. The rotational biases and reversal frequencies were measured for wild type and each of the TnG mutants in the Δ*cheRB* strain HCB436. Cells expressing the T1G, T2G, or T3G protein were all CCW locked, with no reversals being observed for cells expressing any of them (Figure 9B). Apparently, the QEQE level of covalent modification is inadequate to rescue the ability of the mutant proteins to support CW flagellar rotation.

Replacing the native MLLT sequence with variable numbers of Gly residues. One might argue that the added Gly residues in the TnG series of proteins might simply loop out from what could remain a continuous helix running from the MLLT sequence through Pro-219 and beyond. Therefore, residues Met-215, Leu-216, Leu-217, and Thr-218 were replaced with different numbers of Gly residues, a treatment that might alter the TM2- HAMP connection more drastically by completely removing the structural constraints that the transmembrane-sensing domain normally exerts on HAMP. The first construct replaced the MLLT sequence with four Gly residues to yield the 4G variant. Additional variants were made by adding Gly residues in single steps to create the 5G to 9G proteins and deleting Gly residues one at a time to generate the 3G through 0G proteins (Figure 12).

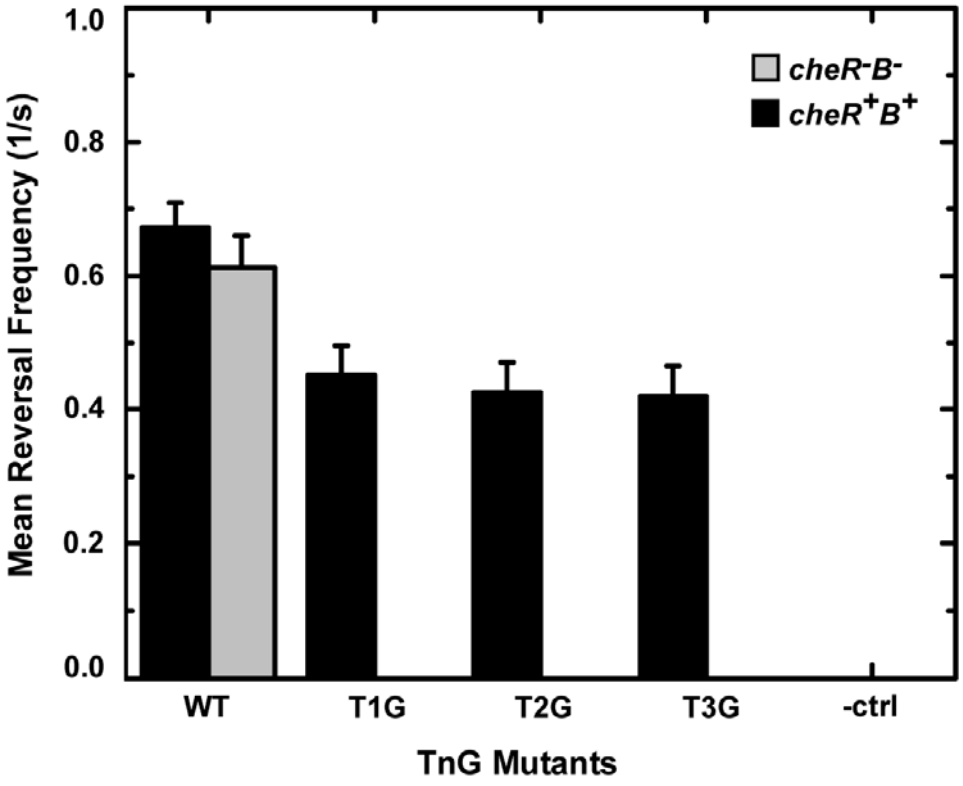

Figure 10. Mean reversal frequencies of cells expressing the TnG mutant receptors. Reversal frequencies were recorded for each strain. Mean frequencies are expressed as reversals/sec, with a reversal defined as a single change in direction (CW → CCW or CCW → CW). Data for cells with intact adaptation machinery (*cheR*$^+$*B*$^+$) are shown in black, whereas data for Δ*cheRB* cells are shown in gray. The error bars represent the standard deviation of the mean, with n=100.

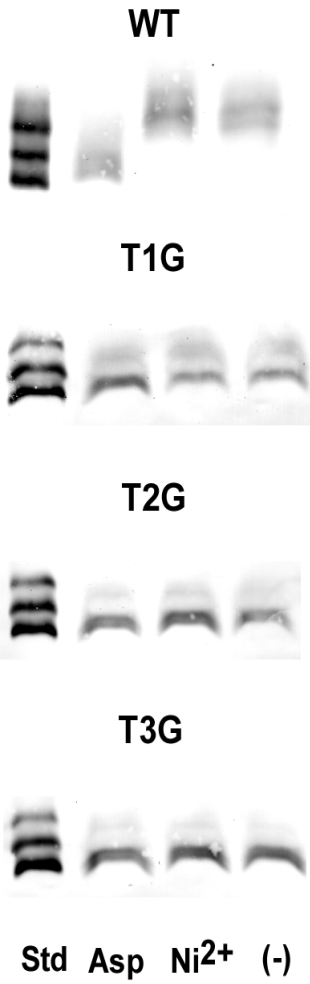

Figure 11. Adaptive methylation of the TnG mutant receptors *in vivo*. *In vivo* methylation levels of Tar were determined in VB13 cells expressing wild-type or TnG mutant receptors from pMK113CV5 after 20 min exposure to 1 mM aspartate, 10 mM Ni^{2+}, or buffer. The methylation state of the receptor is indicated by the rate of migration during SDS-PAGE, with the more-highly methylated receptor forms migrating faster. Migration standards of the EEEE, QEQE, and QQQQ forms of wild-type receptor were loaded in the left lane. The QQQQ form mimics the fully methylated receptor and migrates faster than the QEQE form, and the QEQE form migrates faster than the EEEE form. The proteins were detected using anti-V5 primary antibody and visualized using goat-anti-mouse secondary antibody conjugated to an alkaline phophatase.

The ability of the MLLT-G replacement proteins to mediate chemotaxis. The effect of the substituted Gly residues on the Tar TM2-HAMP junction was first assessed by the rate of chemotactic-ring formation of VB13 cells expressing the different variant Tar proteins in minimal semi-solid agar. The 4G mutant had ~80% of the wild-type rate of aspartate ring expansion (Figure 13). Aspartate taxis decreased in a stepwise manner as Gly residues were subtracted or added. The most extreme mutations, such as -3G, -4G, and +5G, exhibited a complete loss of chemotaxis ability, since plasmids expressing those proteins did not support ring expansion significantly better than the vector control. Maltose chemotaxis and aerotaxis exhibited similar trends as the aspartate taxis.

Rotational biases and the mean reversal frequencies of MLLT-G replacement mutants in a cheR$^+$B$^+$ *strain.* The baseline signaling states supported by the different Tar variants were measured by examining tethered cells. The 4G mutant had rotational characteristics very similar to those of cells expressing wild-type Tar. However, as additional Gly residues were added or subtracted, cell rotation became increasingly CCW biased, and the -3G, -4G, and +5G mutants became CCW locked (Figure 14).
The 4G and 5G proteins yielded MRF values of 0.577 and 0.518 reversals/sec, respectively, not much lower than the MRF value of 0.672 obtained with wild-type cells. The MRF values decreased progressively as more Gly residues were added (6G through 8G) or subtracted (3G and 2G) (Figure 15).

Adaptive methylation of the MLLT-G replacement proteins in vivo*.* The *in vivo* methylation state of the various Tar proteins was measured in VB13 cells expressing the V5-tagged variants of the mutant proteins. All of the Gly variants were overmethylated

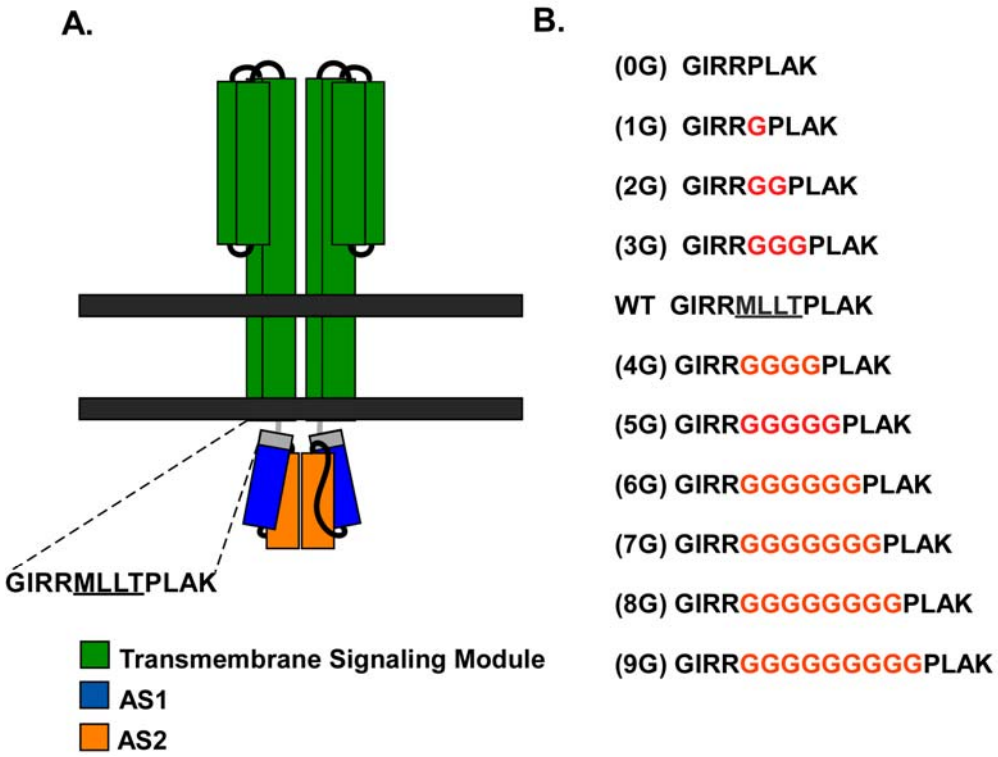

Figure 12. Replacing the native TM2-HAMP connector sequence with multiple Gly residues. (A) A cartoon of the transmembrane-signaling module (green rectangles,) which is connected to AS1 (blue rectangles) and AS2 (orange rectangles) through the TM2-HAMP junction (gray rectangles). The transmembrane-signaling module contains the periplasmic ligand-binding domain and transmembrane helices 1 (TM1) and 2 (TM2), which traverse the membrane. AS1 is a predicted to be a helical extension of TM2 that is connected to AS2 through a flexible connector. (B) The wild-type sequence of the C-terminal end of TM2, the TM2-HAMP junction, and the N-terminus of AS1 are depicted. The 4G mutant has the wild type TM2-HAMP junction sequence (Met-215, Leu-216, Leu-217, and Thr-218) replaced with four Gly residues. The longer and shorter Gly insertion mutants are also depicted. Inserted Gly residues are colored red.

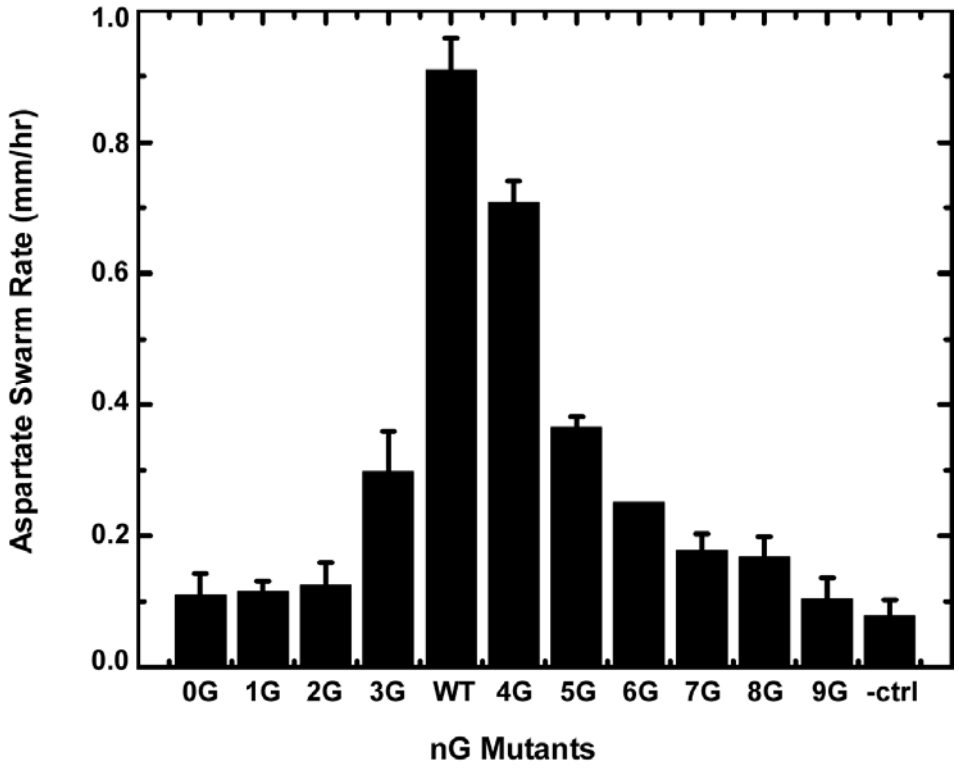

Figure 13. The aspartate chemotaxis-ring expansion rates of cells expressing the nG mutant receptors. The rate at which the chemotaxis-ring diameter increased, measured in mm/h, was measured in VB13 cells expressing wild-type or mutant receptors from pMK113CV5. The error bars represent the standard deviation of the mean, with n=3.

relative to wild-type Tar except for the 2G protein, which was undermethylated, and the 1G protein, which was truncated and presumably totally non-functional. The 0G protein, in which TM2 is joined directly to the Pro residue in AS1 of HAMP, was relatively stable and overmethylated (Figure 16).

Signaling defects of the Gly replacement mutants are exaggerated in the absence of the adaptation machinery. Reversal frequencies and rotational biases were observed in HCB436 cells, which lack CheR and CheB, to observe the effects of removing the compensating effects of the adaptation machinery on the baseline signaling state of the receptor. In these cells, all of the Tar proteins remain in the QEQE form in which they are translated (data not shown). All of the cells, except those expressing the 4G and 0G variants, were locked CCW (Figure 17). The 4G mutant was also overwhelmingly CCW biased, with only 3 cells out of 100 reversing to give a mean MRF of 0.032 reversals/sec for the all the cells tested. The 0G mutant exhibited a less CCW-biased phenotype than the 4G mutant and had an MRF value of 0.34 reversals/sec, about half of the wild-type value.

Discussion

The mechanism by which the signal transmitted across the cell membrane by TM2 is communicated to the HAMP domain to modulate CheA kinase activity remains elusive. To address this question, we used two different sets of mutants to examine the effects of manipulating the secondary structure and the length of the TM2-HAMP junction. Our working hypothesis was that increasing the length and flexibility of the

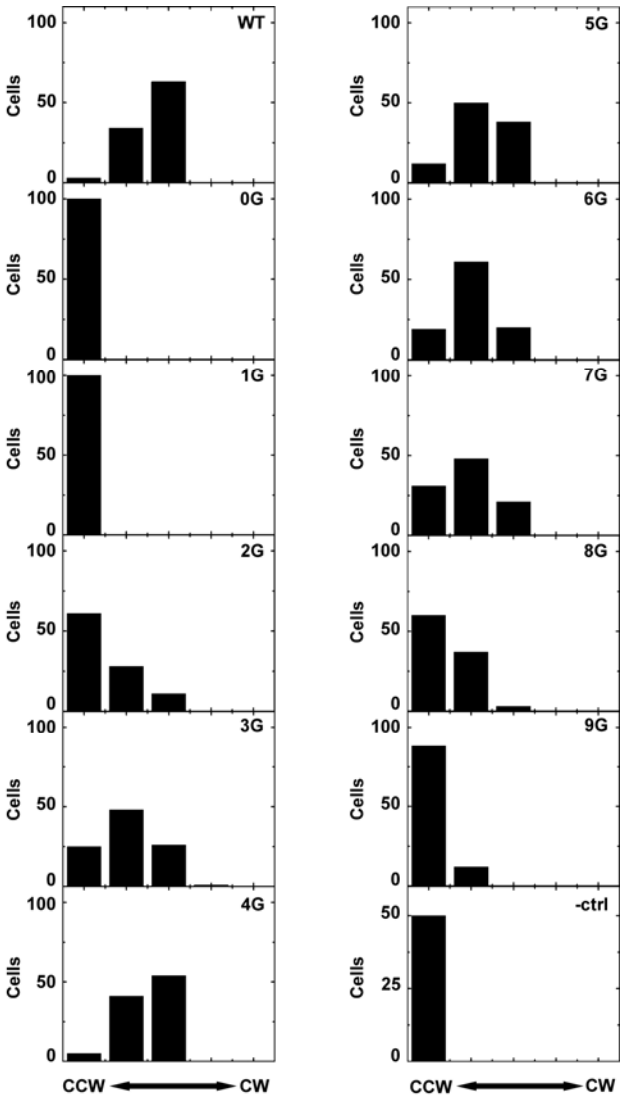

Figure 14. Rotational biases of flagella of tethered cells expressing nG mutant receptors in strains with the adaptive methylation machinery. Transducer-depleted, methylation-competent cells (VB13) expressing wild-type or nG mutant receptors were tethered, and their flagellar rotation was monitored over a 30 sec interval. The cells were placed into one of five categories based on their CW/CCW rotational biases: CCW locked, CCW biased, CCW/CW, CW biased, and CCW locked (graphically depicted above from left to right). One hundred cells were measured for each strain.

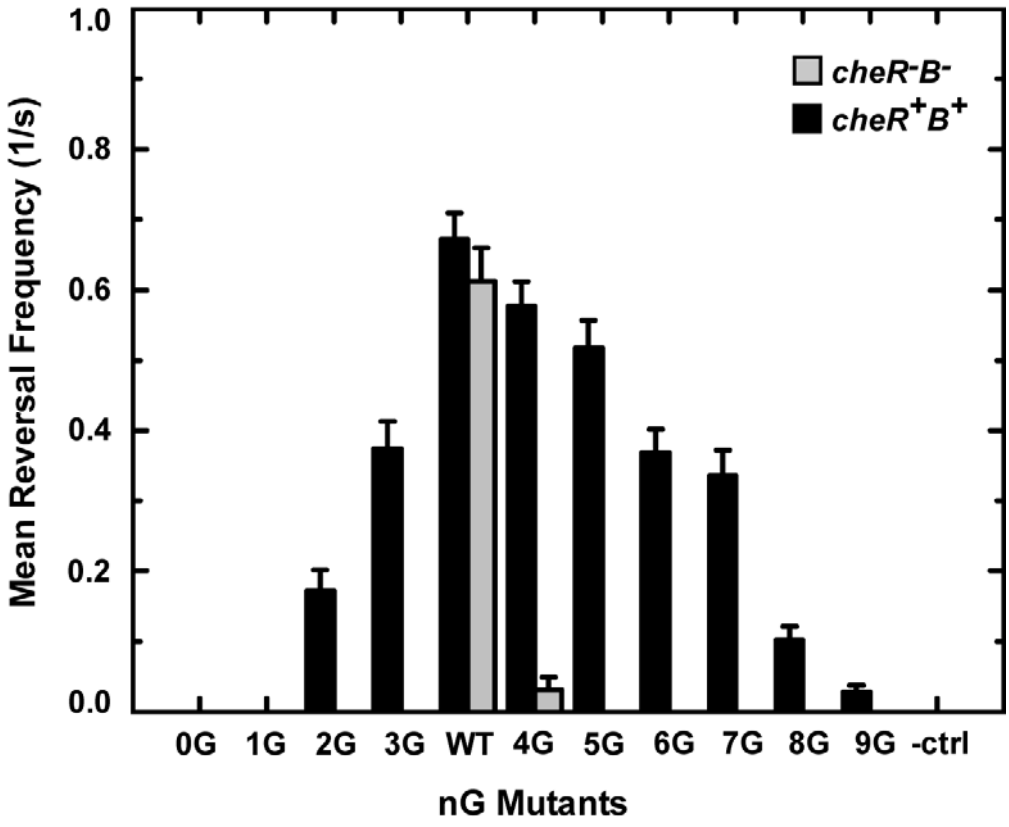

Figure 15. Mean reversal frequencies of cells expressing the nG mutant receptors. Reversal frequencies were recorded for each strain. Mean frequencies are expressed as reversals/sec, with a reversal defined as a single change in direction (CW → CCW or CCW → CW). Data for cells with intact adaptation machinery (*cheR*$^+$*B*$^+$) are shown in black, whereas data for Δ*cheRB* cells are shown in gray. The error bars represent the standard deviation of the mean, with n=100.

connection between TM2 and HAMP could serve to uncouple the transmembrane-sensing domain from HAMP and the kinase-control domain.

An NMR structure of the HAMP domain of the Af1503 transmembrane protein of unknown function from *Archaeoglobus fulgidus* was published in 2006 (*78*). Modeled on that structure, the MLLT sequence in *E. coli* Tar that intervenes between the cytoplasmic end of Tar TM2 (the WYGIRR sequence at residues 209-214) and Pro-219 of AS1 should be able to assume a helical conformation in an intact HAMP domain. In the isolated Af1503 HAMP, this helix is continuous with the remainder of AS1 in the structure, and the Pro-219 residue packs against the N-terminal end of AS2 in the HAMP parallel four-helix bundle (see Figure 5 in Chapter I). However, the strong conservation of Pro at this position in a wide variety of HAMP domains suggests that it plays an important role. Based on the effect of Pro residues in other helices, it could confer a "kink," or abrupt turn, at the N-terminal end of AS1 in at least one possible conformation of the HAMP domain. The possibility cannot be excluded that isomerization of this Pro residue between its *cis* (helix-breaking) and *trans* (helix compatible) forms might play an important role in transmembrane signaling

Insertion of Gly residues. The mechanism by which TM2 and HAMP communicate was first probed by inserting 1, 2, or 3 Gly residues between the MLLT sequence and Pro219 to generate the T1G to T3G (TnG) series of Tar variants. We reasoned that these potentially helix-breaking substitutions might compromise communication between TM2 and HAMP. In general, the results supported our expectations. Inserting even one Gly residue between Thr-218 and Pro-219 drastically

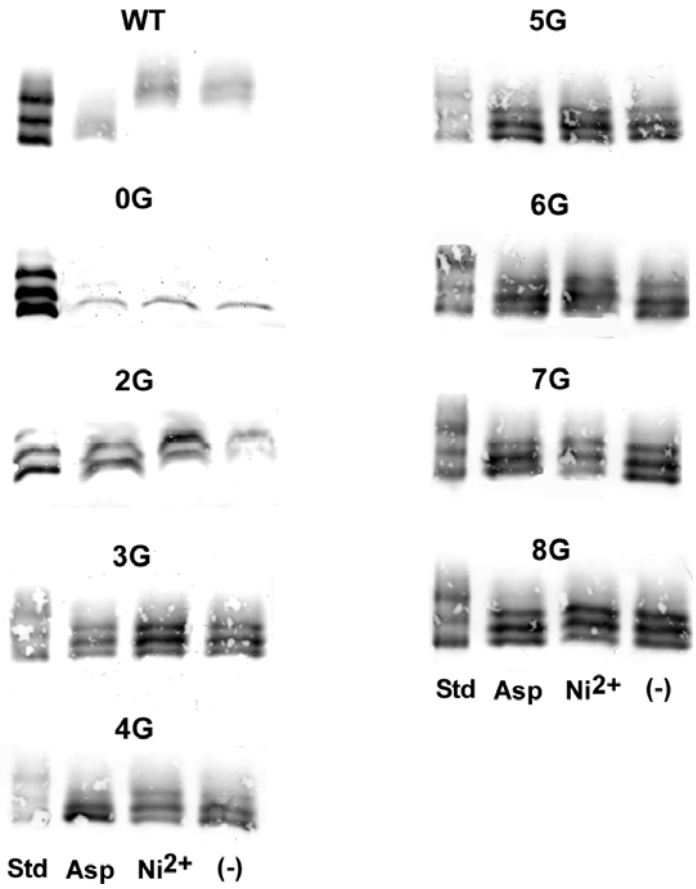

Figure 16. Adaptive methylation of the nG mutant receptors *in vivo*. *In vivo* methylation levels of Tar were determined in VB13 cells expressing wild-type or TnG mutant receptors from pMK113CV5 after 20 min exposure to 1 mM aspartate, 10 mM Ni^{2+}, or buffer. Migration standards were as in Figure 11.

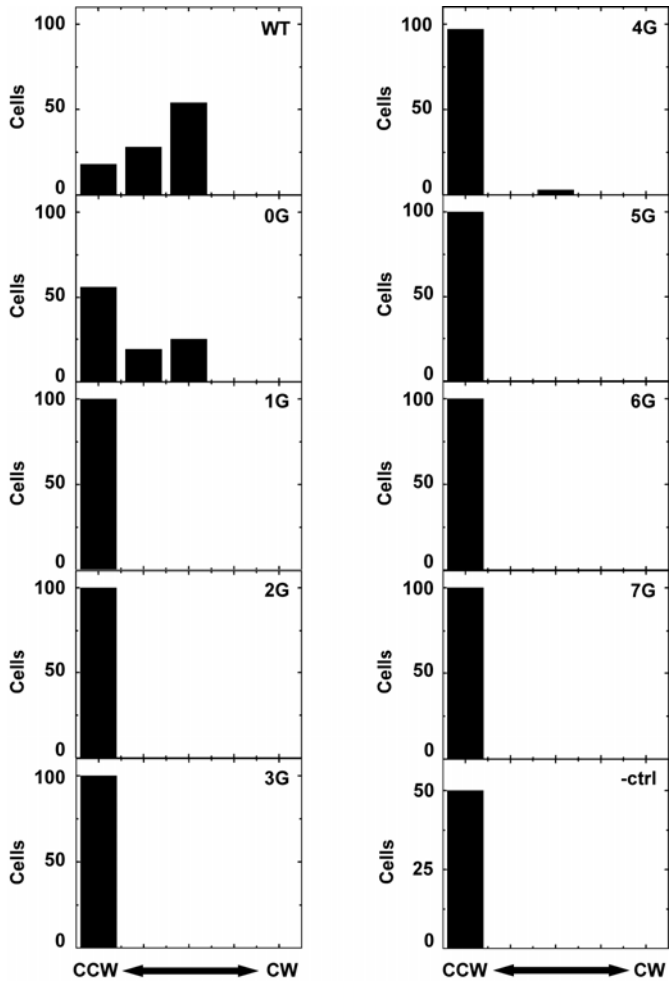

Figure 17. Rotational biases of cells expressing nG mutant receptors in a strain lacking adaptive methylation machinery. The rotational biases were determined over a 30-sec interval in cells lacking the adaptive methylation machinery (HCB436). The cells were classified as described previously, with one hundred cells monitored for each strain.

reduced the ability of the modified protein to mediate aspartate chemotaxis, and insertion of one or two additional Gly residues did not seem to make the situation much worse.

None of these changes destabilized the affected proteins. To a significant extent, adaptive methylation in *cheR*$^+$*B*$^+$ cells could reverse the CCW-locked phenotype associated with these proteins in a Δ*cheRB* cell, in which Tar remains in the QEQE state, and all three mutant proteins were overmethylated in *cheR*$^+$*B*$^+$ cells. The general conclusion is that the ability of the transmembrane-sensing domain to override the inhibitory effect of HAMP on the CheA-kinase stimulating activity of the kinase-control domain is largely abrogated by the Gly insertions. However, the uncoupling is not complete, because the TnG proteins can still mediate aspartate taxis to some degree, and they do change their methylation levels in response to attractant and repellent signals. This result seems inconsistent with the idea that a rotation of TM2 within the membrane is propagated directly to HAMP. Thus, the simplest model to explain the mechanism of transmembrane signaling via direct rotational coupling of TM2 and AS1 via rotation about a continuous helical axis seems unlikely to be correct.

Replacement of the MLLT sequence with Gly residues. The second approach to investigating the TM2-HAMP connection was to remove the MLLT sequence completely and replace it with different numbers of Gly residues to create the nG series of Tar mutants. This approach introduced two additional variables: 1) the importance of the inferred MLLT helical connector between TM2 and Pro-219 could be examined; 2) the effect of the absolute number of residues between TM2 and Pro-219 could be assessed. Some of the results from this analysis were unanticipated.

The first surprise was that the 4G variant, which contains the same number of residues between TM2 and Pro-219 as wild-type Tar, functioned quite well in both chemotaxis (80% of the wild-type aspartate ring diameter) and baseline signaling (very nearly the wild-type rotational bias for tethered cells). Addition or deletion of additional Gly residues deteriorated all aspects of receptor function, although only the 1G variant appeared to be substantially less stable than wild-type Tar. The ability of the proteins to support rotational reversals in tethered *cheR*$^+$*B*$^+$ cells was, as expected, strongly correlated with their chemotactic ability. Most of the proteins were overmethylated in unstimulated cells, the exceptions being the unstable 1G variant and the 2G variant, which, despite its CCW bias, was undermethylated. The latter result suggests that a CCW signaling bias and increased adaptive methylation can be uncoupled in a particular mutant receptor.

HCB436 (Δ*cheRB*) cells expressing the majority of the MLLT-G replacement proteins were CCW locked. In these cells, the receptors should remain in the QEQE state of covalent modification in which they are translated. This level of covalent modification is obviously insufficient to allow significant CW signaling, although increased covalent modification through methylation is adequate to foster CW signaling by several of these proteins. Remarkably, Δ*cheRB* cells expressing the 0G variant were not CCW locked and exhibited nearly the same rotational bias as cells expressing wild-type Tar. This result is peculiar in that the 0G protein was overmethylated in *cheR*$^+$*B*$^+$ cells, but the cells were still CCW locked. This finding provides a second example of deviation from the canonical connection between receptor signaling and covalent modification states.

Previous studies (*57, 58*) have shown that cells expressing receptor fragments containing the cytoplasmic signaling and adaptation domains are constitutive CW signalers. *In vitro* experiments (*91, 92*) have also shown that when such fragments are mixed with CheW and CheA, kinase activity increases several hundred-fold over its level in their absence. A similar fragment containing the HAMP domain has less CheA-stimulating ability than the fragment containing the signaling and adaptation domains (J. S. Parkinson personal communication). Addition of the transmembrane-sensing domain to this fragment reverses the inhibition of kinase activity by HAMP. The simplest interpretation of the results reported here is that increasing the length and flexibility of the TM2-HAMP connection tends to uncouple signal propagation between those two elements to approach the signaling behavior shown by the soluble HAMP-kinase-control fragment. However, in most cases increased adaptive methylation can reverse this effect and some level of normal communication between attractant and repellent binding to the periplasmic domain and regulation of kinase-stimulating function.

The "frozen-dynamic" model for chemoreceptor signaling suggests that the allosteric inputs modulate the dynamics of the CD1-CD2 four-helix bundle. In the kinase inhibiting (attractant-bound) state, the four-helix bundle becomes more dynamic, whereas in the kinase-activating (repellent-bound) state the four-helix bundle becomes less dynamic (*22, 93*). Covalent modification of glutamyl residues in the adaptation subdomain neutralizes their negative charge, decreasing the electrostatic repulsion between subunits within the four-helix bundle and stabilizing it (i.e., making it less dynamic) (*70, 88*). This model potentially explains how increased methylation can

compensate for increased CCW signaling. Introducing flexibility into the TM2-HAMP junction may stabilize the conformation of the HAMP domain that destabilizes the CD1-CD2 four-helix bundle. The underlying principle is that the HAMP domain in an unstimulated receptor must be maintained at an intermediate stability to enable it to respond to both attractant and repellent signals. Input from the transmembrane-sensing domain and the adaptation subdomain both work to achieve this balance.

This relatively simple model is complicated by the aberrant behavior of the 0G and 2G proteins, in which the normal connection between the extent of covalent methylation and signaling state is altered. Possible interpretations of their behavior and a consideration of what they may tell us about receptor structure-function relationships will be considered in the general discussion in Chapter IV.

CHAPTER III

THE EFFECT OF CHANGING THE HELICAL REGISTER OF THE TM2-HAMP JUNCTION

Introduction

Chapter II described experiments in which varying numbers of glycyl residues, which should break helicity of the polypeptide chain, were introduced into the TM2-HAMP junction region of the *E. coli* aspartate/maltose chemoreceptor Tar. In this chapter we consider different modifications of this region in which residues were added or deleted from the MLLT sequence in the TM2-HAMP connector that would be expected to retain the helicity of this region. This effort was undertaken to determine whether the predicted helical register of the MLLT sequence is an important component of the propagation of the transmembrane signal from TM2 to the HAMP domain.

The most crucial residue in this sequence appears to be the second one, Leu-216. Changes of the Leu residue at the equivalent position in the TM2-HAMP linker of the *E. coli* serine receptor Tsr severely disrupted its function, whereas changes at the other three positions, which are not conserved between Tsr and Tar, had little effect (J. S. Parkinson unpublished results). In keeping with this trend, the 1G variant of Tar, which has the MLLTP sequence replaced with MGP, is unstable and non-functional. However, the 0G and 2G Tar variants, in which Pro-219 is joined directly to TM2 or in which TM2 and Pro-219 are separated by two Gly residues, are stable and at least partially

functional, although they show unusual relationships between kinase stimulating activity and covalent modification state.

The conclusion from the work described in this chapter is that changing the helical register of the TM2-HAMP connection has profound effects on Tar function. Receptors in which the connector has roughly the same helical register as it does with the wild-type MLLT sequence are, as a rule, more active than receptors in which the helical register is altered. It appears that both the length and the proper helical register are important for optimal receptor function.

Materials and methods

Bacterial strains and plasmids. The strains and parental plasmids used in this work are identical to those described in Chapter II. Mutations were introduced into the *tar* gene via standard site-directed mutagenesis (Stratagene).

Measuring chemotaxis to attractants. Swarm assays were conducted exactly as described in Chapter II.

Observation of tethered cells. Tethered cells were prepared, observed, and analyzed exactly as in Chapter II.

In vivo *methylation. In vivo* methylation assays were performed exactly as described in Chapter II.

Results

Shortening and lengthening the predicted helical extension between Arg-214 of TM2 and Pro-219 of AS1. To examine the effects of the helical periodicity and length of the TM2-HAMP junction on the communication between TM2 and HAMP, we constructed Tar variants that have shorter or longer predicted helical stretches between Arg-214 and Pro-219 (Figure 18). The shorter constructs have the following residues between Arg-214 and Pro-219: -4, none; -3, M; -2, ML; -1 MLL. The -4 construct is identical to the 0G construct described in Chapter II. The longer constructs contain the following residues between the MLLT sequence and Pro-219: +1, L; +2, LL; +3, LLT; +4, LLTL; +5, LLTLL; +6, LLLTLLT; +7, LLTLLTL; +8, LLTLLTLL.

Aspartate chemotaxis mediated by Tar TM2-HAMP mutants containing shortened or lengthened helical connectors. The effects of the deletions or additions of residues to the TM2-HAMP connector were tested with VB13 cells containing pMK113-derived plasmids expressing the respective variant proteins at near-physiological levels (Figure 19). The -4, -3, and +5 through +8 proteins supported no aspartate taxis, giving chemotaxis swarms indistinguishable from those produced by VB13 cells containing the vector plasmid. Cells expressing the -2 and -1 Tar variants had aspartate chemotaxis rings with 15% and 50% the diameter of rings produced by cells expressing wild-type Tar. Cells expressing the +1, +2, +3, and +4 variants formed aspartate rings with 10%, 20%, 22%, and 35% of the diameter, respectively, of the aspartate rings formed by cells expressing wild-type Tar. The superior performance of cells expressing the +4 variant, which should come closest to restoring the same helical register as the wild-type protein,

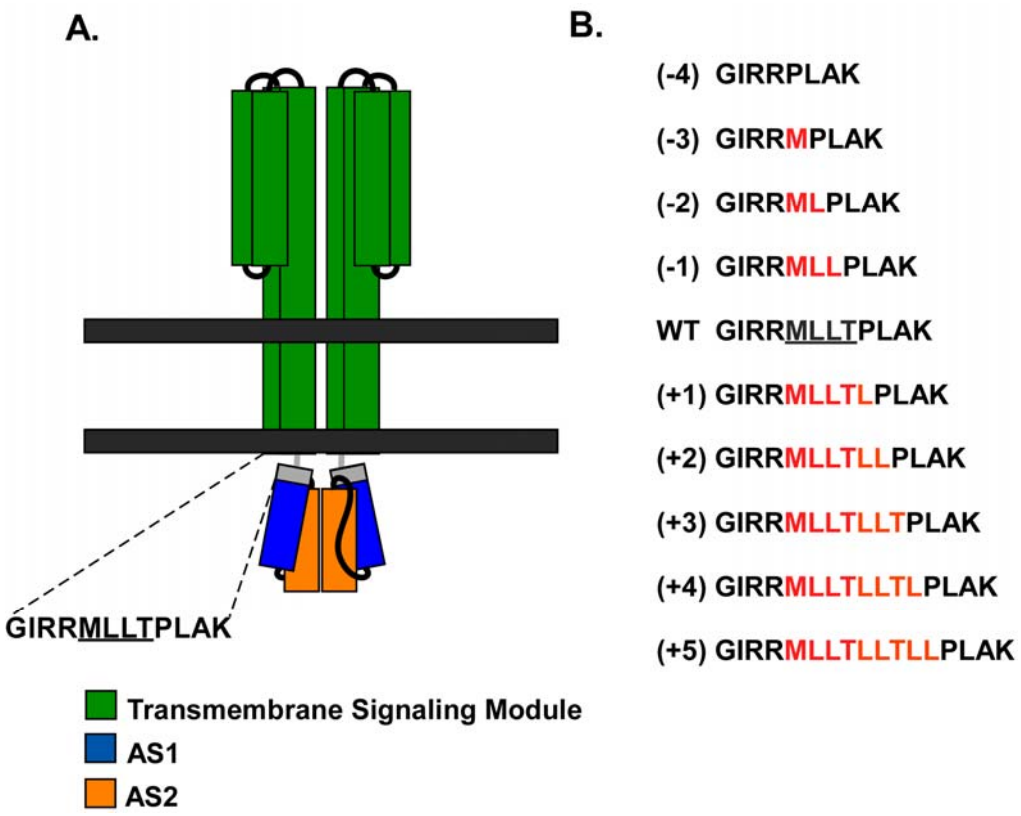

Figure 18. Shortening and lengthening the helical extension between Arg-214 and Pro-219. (A) A cartoon of the transmembrane-signaling module (green rectangles), which is connected to AS1 (blue rectangles) and AS2 (orange rectangles) through the TM2-HAMP junction (gray rectangles). The transmembrane-signaling module contains the periplasmic ligand-binding domain and transmembrane helices 1 (TM1) and 2 (TM2), which traverse the membrane. AS1 is a predicted helical extension of TM2 that is connected to AS2 through a flexible connector. (B) The wild-type sequence of the C-terminal end of TM2, TM2-HAMP junction, and the N-terminus of AS1 are depicted. The red letters show the residues that were present at the TM2-HAMP junction.

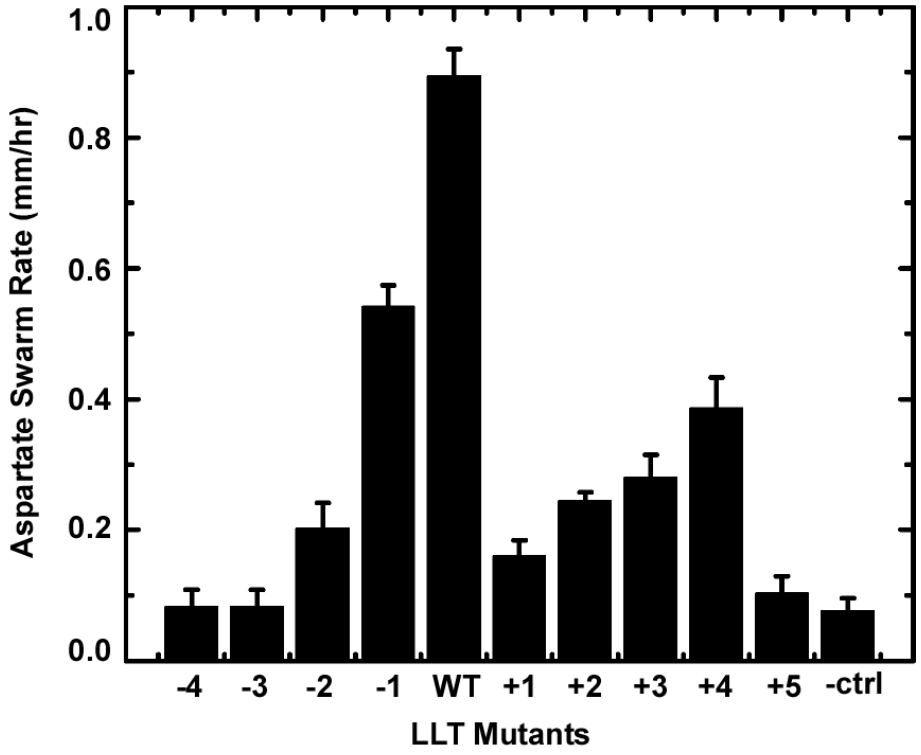

Figure 19. The aspartate chemotaxis-ring expansion rates of cells expressing the LLT mutant receptors. The rate at which the chemotaxis-ring diameter increased, measured in mm/h, was measured in VB13 cells expressing wild-type or mutant receptors from pMK113CV5. The error bars represent the standard deviation of the mean, with n=3.

was notable. There was also no indication of the symmetrical decay in aspartate chemotaxis behavior shown by cells expressing proteins shorter or longer than the 4G variant described in Chapter II. Maltose chemotaxis and aerotaxis exhibited similar trends as aspartate chemotaxis.

Rotational biases and mean reversal frequencies of Tar TM2-HAMP mutants containing shortened or lengthened helical connectors. To examine the effects of shortening or lengthening the TM2-HAMP junction on the baseline signaling activity of the receptor, we measured the rotational biases and mean reversal frequencies of the -4 through +8 variants in VB13 cells (Figure 20 and 21). One hundred cells were measured for the wild-type and each mutant receptor. Cells expressing wild-type Tar made frequent reversals between CW and CCW rotation, as seen previously. The -4, -3, +6, +7, and +8 variants showed CCW locked rotation. Cells making the -1 protein, which supported the best chemotaxis among the mutant variants, exhibited a nearly wild-type rotational bias, being only slightly more CCW biased. The remaining mutant proteins showed a strong correlation between their ability to generate CW rotation and their ability to support aspartate taxis. Cells producing the -2 and +2 proteins were more CCW biased than cells expressing the +3 and +4 proteins but less CCW biased than cells producing the +1 protein. The CCW bias of the +3and +4 mutants was similar and somewhat greater than for -1 or wild-type Tar.

The mean reversal frequency (MRF) of cells expressing wild-type Tar was 0.60 reversals/sec. The -1 mutant had a MRF value of 0.55 reversals/sec. The MRF values for cells expressing the -2, +1, +2, +3, +4, and +5 mutant proteins were 0.25, 0.2, 0.35, 0.4,

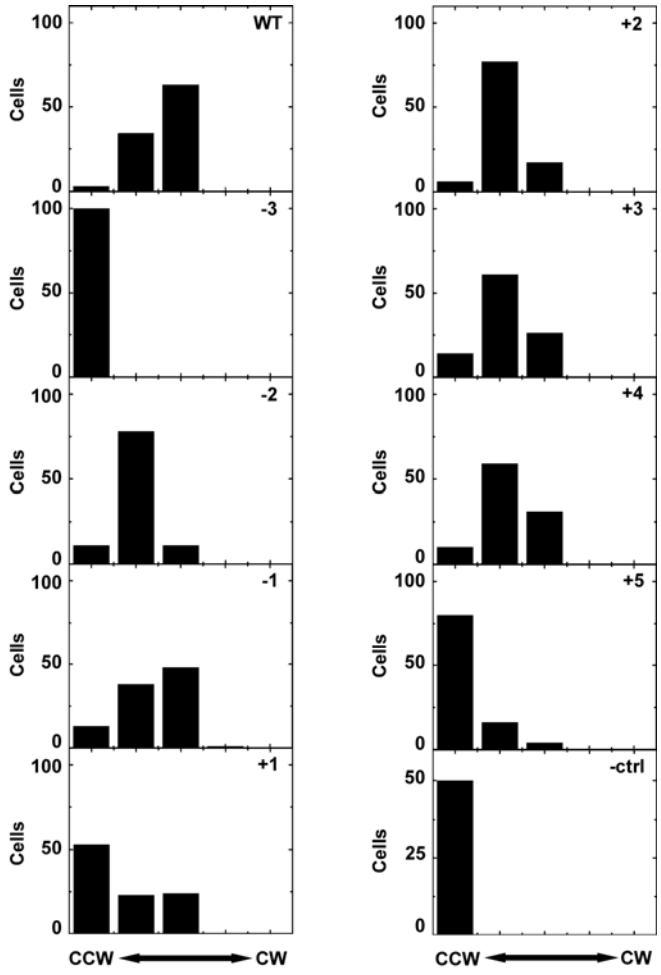

Figure 20. Rotational biases of flagella of tethered cells expressing LLT mutant receptors in strains with the adaptive methylation machinery. Transducer-depleted, methylation-competent cells (VB13) expressing wild-type or nG mutant receptors were tethered, and their flagellar rotation was monitored over a 30 sec interval. The cells were placed into one of five categories based on their CW/CCW rotational biases: CCW locked, CCW biased, CCW/CW, CW biased, and CCW locked (graphically depicted above from left to right). One hundred cells were measured for each strain.

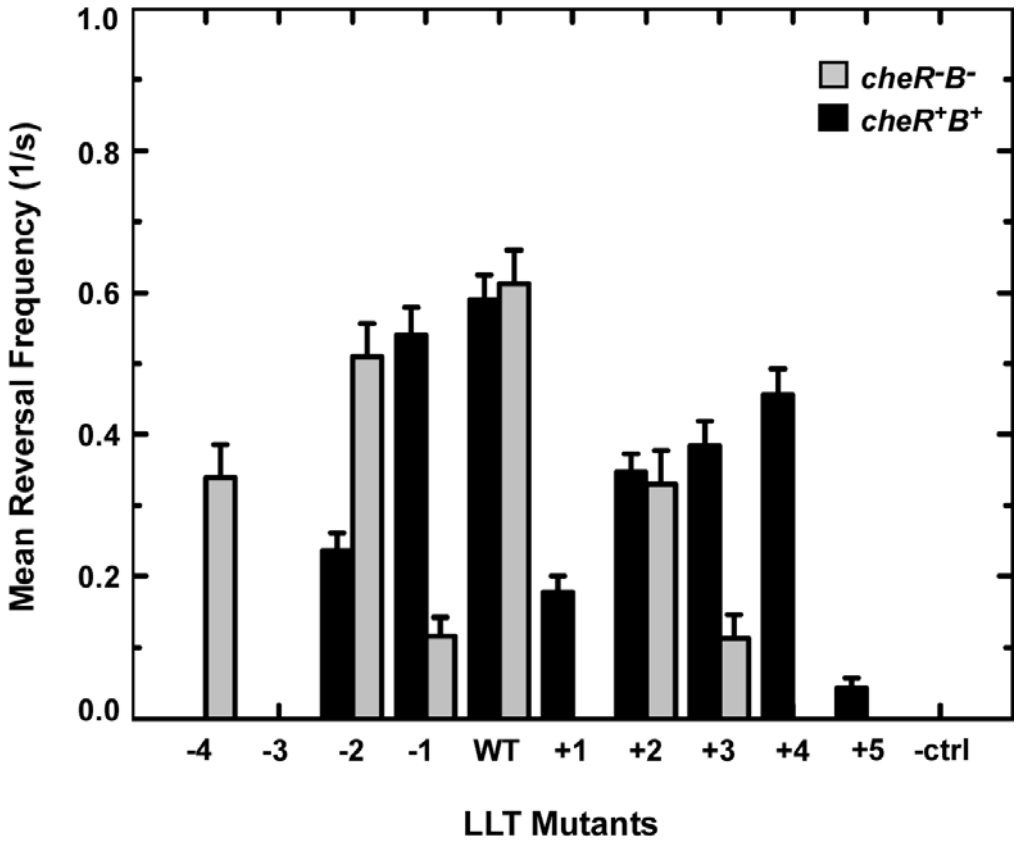

Figure 21. Mean reversal frequencies of cells expressing the LLT mutant receptors. Reversal frequencies were recorded for each strain. Mean frequencies are expressed as reversals/sec, with a reversal defined as a single change in direction (CW → CCW or CCW → CW). Data for cells with intact adaptation machinery (*cheR*$^+$*B*$^+$) are shown in black, whereas data for Δ*cheRB* cells are shown in gray. The error bars represent the standard deviation of the mean, with n=100.

0.45, and 0.05, respectively. These MRF values closely reflect the degree of chemotaxis and the CW/CCW rotational bias supported by the various proteins.

Adaptive methylation of the Tar TM2-HAMP mutants containing shortened or lengthened helical connectors in vivo. The methylation states of the -4 through +8 mutants were measured in strain VB13 (Figure 22). Methylation levels of wild-type Tar receptor were similar to those seen previously in the unstimulated state and after the addition of L-aspartate or $NiSO_4$. No bands were seen with the -3 and +5 through +8 proteins, which are presumably unstable and/or not inserted into the membrane. The -1 mutant showed methylation patterns very similar to those of the wild-type protein but was slightly more methylated in the unstimulated state. The +1, +4, and -4 proteins were over-methylated compared to wild-type Tar but still showed the appropriate responses to aspartate and Ni^{2+}. The +2 and +3 mutants maintained an intermediate level of methylation that did not change upon addition of aspartate or $NiSO_4$. The -2 mutant was noticeably undermethylated relative to wild-type Tar, and it did not change its methylation level with the addition of aspartate or $NiSO_4$.

Signaling defects in most of the deletion and extension mutants are exaggerated in the absence of the adaptation machinery. We also measured the rotational bias and MRF values of Δ*cheRcheB* cells expressing the various mutants Tar proteins (Figures 23 and 21). One hundred cells each were monitored for cells expressing the wild-type and mutant receptors. Cells expressing wild-type Tar had similar rotational biases and MRF values as VB13 cells expressing wild-type Tar, except that a somewhat higher percentage of cells were CCW locked. Cells expressing the +1, +4, and +5 variants were

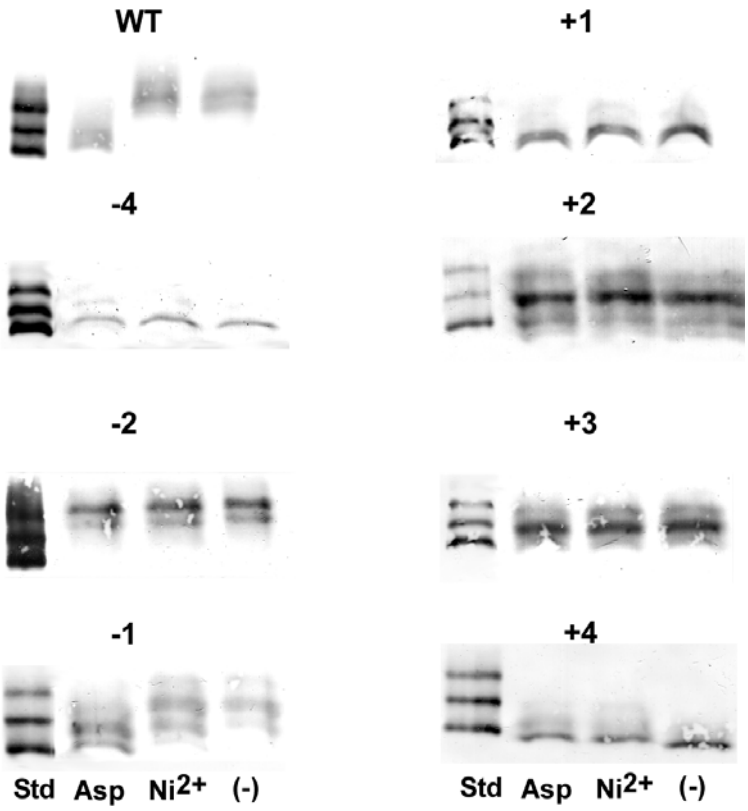

Figure 22. Adaptive methylation of the LLT mutant receptors *in vivo*. *In vivo* methylation levels of Tar were determined in VB13 cells expressing wild-type or LLT mutant receptors from pMK113CV5 after 20 min exposure to 1 mM aspartate, 10 mM Ni^{2+}, or buffer. Migration standards were as in Figure 11.

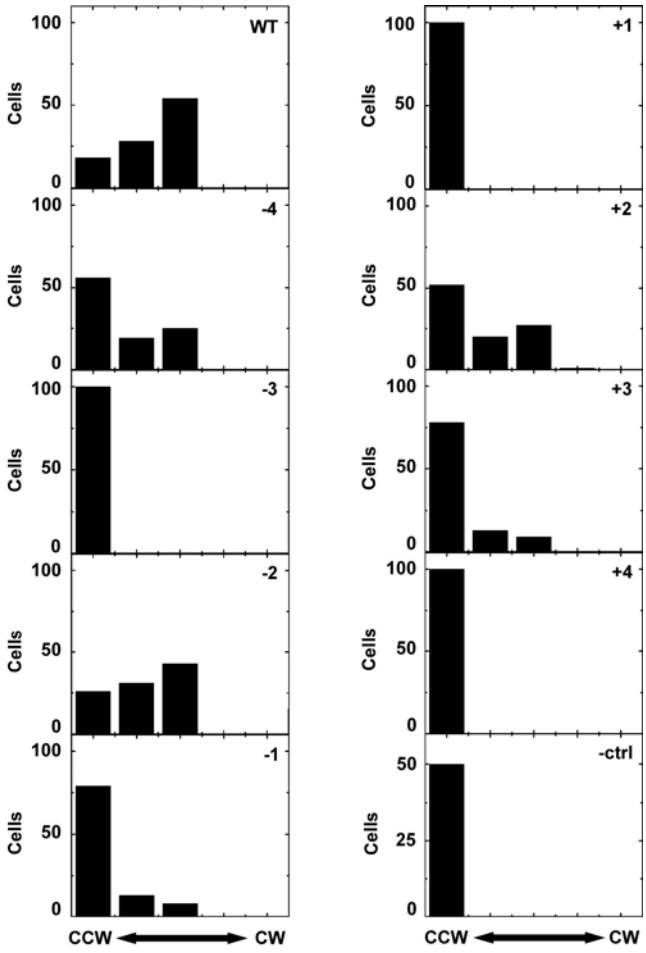

Figure 23. Rotational biases of cells expressing LLT mutant receptors in a strain lacking adaptive methylation machinery. The rotational biases were determined over a 30-sec interval in cells lacking the adaptive methylation machinery (HCB436). The cells were classified as described previously, with one hundred cells monitored for each strain.

CCW locked. The result with the +4 mutant is particularly striking, since cells expressing that protein showed reasonably good chemotaxis. Cells expressing the -1 and +3 variants were severely CCW biased. Cells expressing the +2 protein were less CCW biased than cells expressing the -1 and +3 proteins but more CCW biased than cells expressing wild-type Tar. Remarkably, cells producing the -2 Tar variant were only modestly more CCW biased than wild-type cells. As with the identical 0G mutant discussed in Chapter II, cells expressing the -4 receptor were CCW biased but still able to reverse.

The MRF for cells expressing wild-type Tar in the Δ*cheRB* strain was 0.60 reversals/sec. Cells expressing the -4, -2, -1, +2, +3, and +4 mutant proteins, all of which were present in reasonable amounts, had MRF values of 0.34, 0.50, 0.11, 0.35, 0.11, and 0 reversals/sec, respectively. Unlike *cheR*$^{+}$*B*$^{+}$ cells expressing these mutant proteins, no clear correlation between the helical periodicity of the TM2-HAMP junction and the MRF is apparent. Thus, the critical parameter of a Tar protein's ability to function in aspartate taxis is its ability to support flagellar reversal in a cell that can carry out compensatory adaptive methylation to offset an intrinsic signaling bias.

Discussion

The results presented in Chapter II argue that both the length and flexibility of the TM2-HAMP connector are important factors in setting the signaling state of Tar. They also argued that even receptors with intrinsically CCW-locked signaling could, in most cases, be made capable of kinase-stimulation by virtue of increased methylation by

the adaptation system. Furthermore, even with longer and/or more flexible (i.e., Gly-rich) connectors, some aspartate chemotaxis was retained, indicating that ligand-induced conformational changes could still be transmitted, although perhaps in attenuated form, to the kinase-control domain. No clear evidence for the importance of helical periodicity was obtained. The most crucial feature of the connector seemed to be its total length, since the protein in which the four-residue MLLT sequence was replaced with GGGG behaved the most like wild-type Tar.

A rather different picture emerges when residues are subtracted from or added to what should remain a helical connector. Although the -1 (MLL) receptor retained the ability to support reasonably good aspartate taxis and CW flagellar rotation, the +1 receptor was very poor at supporting aspartate taxis, and *cheR*$^+$*B*$^+$ cells expressing either the +1 and +2 receptors were very CCW biased. Given a 100^o rotation per residue in a free helix, the +3 and +4 receptors come within 60^o and exceed by 40^o restoration of the helical register of the connector. These proteins were significantly better at supporting chemotaxis and CW flagellar rotation than the +1 and +2 receptors. Thus, the helical register seems to be an important consideration. However, length clearly is also important, because the +5 through +8 receptors were not detected by immunoblotting, even though the +7 receptor should come within 20^o of restoring the proper helical register. It seems likely that, in these proteins, the HAMP and or kinase-control domains may be simply too far away from the cell membrane to allow proper assembly of the receptor dimers or trimers of dimers.

The -3 receptor has only one residue between TM2 and the conserved Pro-219 was unstable and non-functional, like the 1G mutant in the previous chapter. In both proteins, the critical Leu-216 residue is absent, although the partial function of the 2G Tar variant, which also lacks Leu-216, suggests that this residue is not absolutely essential to achieve some level of receptor function.

Taken together, the results presented here and in Chapter II suggest the following properties about the TM2-HAMP connector. 1) It is important that the connector be of the correct length – four residues. This is particularly true when the connector is made up in part, or entirely, of Gly residues, since the 3G variant is much less active than the -1 (MLL) variant, although both have a three-residue connector.

2) Shortening the connector does not automatically lead to a CW-biased signal output. It has been previously observed (*68*) that moving the aromatic Trp-209/Tyr-210 anchor at the cytoplasmic hydrophobic/hydrophilic interface of Tar TM2 in the N-terminal direction increases CCW signal output. Moving the Trp-209/Tyr-210 anchor in the C-terminal direction increases the CW signal output. These findings were interpreted as meaning that moving the Pro-219 farther from the aromatic anchor favors CCW signaling and moving Pro-219 closer to the aromatic anchor favors CW signaling. However, none of the shortened connectors studied here increased CW signal output, although they should bring Pro-219 closer to the aromatic anchor. Thus, the simplest interpretation of the earlier work is not correct. Of course, it could be that shortening the connector directly distorts the conformation of the HAMP domain in some way that moving the aromatic anchor does not.

3) The helical periodicity of the connector is important for determining signal output if the connector is lengthened, but not if it is shortened. The +4 receptor, which comes within 40^{o} of restoring the proper helical register of the connector, retains reasonably good chemotactic function and supports CW rotation in a *cheR*$^{+}$*B*$^{+}$ strain. It functions much better than the +1 and +2 receptors, although not as well as the -1 receptor. Its behavior is much like that of receptors in which the aromatic anchor was moved in the N-terminal direction (*68*): they also were overmethylated and gave CCW locked rotation in a Δ*cheRB* strain. It could be that if the connector is shortened it loses its ability to pack as a helix and becomes disordered, much like the Gly residues. However, the somewhat different phenotypes associated with the 2G and -2 receptors indicate that the ML linker and 2G linker are not identical.

4) The inputs to the adaptation domain and signaling domain can be uncoupled. Three of the Tar constructs discussed here do not show the typical correlation between rotational bias and extent of covalent modification. i) The first exception is the variant in which the WYIGRR sequence at the C-terminus of TM2 is positioned directly adjacent to the Pro residue of AS1 (the 0G or -4 variant). This protein does not support any aspartate taxis. In a *cheR*$^{+}$*B*$^{+}$ strain, the protein is overmethylated and is CCW locked. However in a Δ*cheRB* strain, this protein is capable of producing a CW signal. This is the only TM2-HAMP junction variant of Tar that is capable of producing a CW signal but incapable of supporting chemotaxis. It may be that the close juxtaposition of Pro-219 to the membrane in this protein does not allow the ligand-induced, piston-like movement of TM2 to be communicated to HAMP.

ii) The second exception is the 2G variant of Tar, which is capable of supporting some level of chemotaxis but gives CCW-locked rotation in its unstimulated state in the Δ*cheRB* cells but becomes capable of CW rotation in a *cheR*$^{+}$*B*$^{+}$ strain. In its unstimulated state, the intrinsic CCW-signaling bias of this receptor does not lead to increased methylation. However, exposure of cells containing this protein to aspartate does generate increased methylation, presumably a prerequisite for these cells to be able to respond to aspartate gradients.

iii) The third exception is the -2 protein, which is in some ways the most puzzling of all. It supports some level of ring expansion in aspartate-minimal semi-solid agar, it is undermethylated in its unstimulated state, its methylation level does not change upon addition of either aspartate or NiSO4, and *cheR*$^{+}$*B*$^{+}$ cells expressing it are CCW biased. However, in its QEQE state, as it is found in Δ*cheRB* cells, it is capable of generating nearly as much CW signal as wild-type Tar. Presumably this protein must still relay conformational changes generated by attractant binding to the transmembrane-signaling domain to the signal-output domain. However, aspartate (or Ni^{2+}) binding have no effect on the adaptation subdomain.

One possible explanation is that whatever distortion is imposed by the -2 mutation has a greater effect on the adaptation subdomain of the receptor than on the kinase control domain. For example, the -2 protein might become a poor substrate for CheR but retain its capacity to be deamidated by CheB. Thus, there would be less electrostatic repulsion within the adaptation subdomain in the QEQE form of the protein present in Δ*cheRB* cells than in the form found in *cheR*$^{+}$*B*$^{+}$ cells. The result would be a

less-dynamic CD1-CD2 four-helix bundle in the Δ*cheRB* cells and a greater extent of CheA kinase stimulation. If this idea is correct, a Δ*cheB* strain expressing the -2 protein should behave like a Δ*cheRB* strain expressing the -2 protein, whereas a Δ*cheR* strain expressing the -2 protein should behave like the $cheR^{+}B^{+}$ strain expressing the -2 protein.

The results reported here and in Chapter II do not solve the problem of how HAMP converts the presumed piston-like transmembrane signal into a change in the dynamics of helical packing in the CD1-CD2 four-helix bundle. However, they do eliminate some possible mechanisms and suggest experiments to test other models for communication between TM2 and HAMP. These issues will be discussed in Chapter IV.

CHAPTER IV

SUMMARY AND CONCLUSIONS

Summary

The HAMP domain is thought to convert the asymmetric signal from the piston-like movement of TM2 into a symmetric signal in the kinase control module. How this signal is communicated through the HAMP is not known. In this dissertation, I address how the TM2-HAMP junction is important in the communication between the TM2 and HAMP and how manipulating the secondary structure and length of this region can disrupt the communication of the TM2 signal into HAMP, thereby interdicting normal regulation of the kinase control module. The results from Chapters II and III suggest the following features of the TM2-HAMP connector are important. 1) The normal length of the TM2-HAMP connector (4 residues) is important for proper receptor function. 2) Shortening the TM2-connector does not result in a CW-locked or CW-biased receptor. 3) The helical periodicity of the TM2-HAMP connector is important for determining signal output only if the connector is lengthened. 4) The inputs from the adaptation to the signaling domain can be uncoupled. In this chapter, I discuss the implications of the mutations affecting the TM2-HAMP junction for our understanding of the control of CheA kinase activity and methylation-dependent adaptation. I will also discuss why some proposed mechanisms for communication between TM2 and HAMP cannot be correct and suggest new experiments to test the other models.

A multi-state frozen-dynamic model for receptor signaling

As discussed in Chapter II, the results obtained with the Gly mutants support the frozen-dynamic model for receptor signaling. In this model, covalent modification by methylation or amidation of certain Glu residues acts as an electrostatic switch to modulate the dynamics of the kinase control domain. A recent mutational analysis of the connector between AS1 to AS2 (*80*) suggests that the CD1-CD2 four-helix bundle can become so tightly packed that it also produces a kinase-inhibiting state. Several of the connector mutants impose a bipolar phenotype such that in the presence of the CheRB adaptation machinery the receptor is CCW biased, whereas in a *ΔcheRB* strain the receptor is CW biased. In those experiments methylation states were not determined, but the suggestion is that there is an optimal packing and stability of the kinase control domain four-helix bundle that elicits a kinase activating receptor. If the four-helix bundle of the kinase control domain is too loosely packed or too tightly packed, kinase activity is inhibited.

The three mutants (0G, 2G, and -2) that show abnormal coupling of the adaptation and signal-output domains complicate the simple frozen dynamic model. My interpretation of the properties of these proteins in the two preceding chapters is that the mutant receptors had differentially altered accessibility to CheR and CheB. As an alternative interpretation, I will discuss other possibilities for the effects of the 0G, 2G, and -2 mutants on the helical packing of the kinase-control domain and consider how the compensatory methylation can affect the signaling state of the mutant receptors.

Cells expressing the 0G receptor were CCW-locked in the presence of the adaptation machinery. In its absence, the cells were not CCW-locked, although they did show a CCW bias relative to cells expressing wild-type Tar. The 0G mutant receptor is also incapable of mediating a chemotaxis response toward aspartate. This suggests that, in the presence of the methylation machinery, the drastic shortening of the TM2-HAMP junction of the unstimulated 0G receptor may cause HAMP to assume a conformation that causes the adaptation subdomain to become overmethylated. This overmethylation, in turn could cause the signal-output domain to pack so tight that it inhibits kinase activation. In the absence of the methylation machinery, no increase in methylation can occur, and the signal-output domain will remain in a conformation that allows some activation of CheA. If this is true, mutations that are thought to destabilize the kinase-control domain, such as the one leading to the R505E substitution in the adaptation domain (*71*), might reverse the CCW-locked phenotype of the 0G mutant.

The 2G receptor produced a CCW-locked phenotype in the absence of the methylation machinery, but its output became less CCW biased in the presence of the methylation machinery. Cells expressing the 2G receptor are capable of some aspartate taxis, and the 2G receptor is undermethylated in a *cheR*$^+$*B*$^+$ strain. In the absence of the methylation machinery, a distorted and essentially inactive HAMP domain allows the kinase-control module to become too tightly packed in the QEQE state, resulting in a kinase inhibiting state and a CCW-locked phenotype. In the presence of CheB, however, deamidation/demethylation of the adaptation domain may loosen the packing of the kinase control module four-helix to create a kinase-activating conformation. Once again,

the prediction would be that the helix-destabilizing R505E substitution might return the QEQE form of the 2G receptor to generate a less CCW-biased output.

In the presence of the methylation machinery, cells expressing the -2 receptor were strongly CCW biased, and the receptor was undermethylated. However, in the absence of the methylation machinery, the -2 (ML) receptor supported CW/CCW rations only slightly more CCW biased than cells expressing wild-type Tar. In this protein, the HAMP domain may be perturbed enough that the kinase-control module becomes slightly overwound in the QEQE state, resulting in a slightly higher CCW bias. In the presence of CheRB, the tighter packing of the kinase control module may evoke deamidation/demethylation of the receptor that causes an overcompensated loosening of the kinase-control module that leads to a further decrease in kinase stimulation. In this case, mutations in the adaptation domain that favor tighter packing (*71*) might decrease the CCW bias seen with the -2 receptor expressed in a *cheR*$^+$*B*$^+$ strain. .

Taken together, these results support a multi-state frozen dynamic model in which HAMP and the kinase-control module must be in an optimal packing of the CD1-CD2 four-helix bundle for maximum kinase activity to be observed. Either too-loose packing or too-tight packing would compromise kinase-stimulation activity. Too-tight packing could elicit a demethylation response that could restore normal CW-CCW output, as with the 2G receptor, or which might overcompensate. The excessively tightly packed state may simply be an overshoot of the tighter packing, increased kinase stimulation, and compensatory demethylation elicited by a repellent with wild-type receptor (Figure 24).

Figure 24. A diagram illustrating a multi-state frozen dynamic model for receptor signaling. The normal distribution bell curve represents the increasing kinase activity of the receptor as a function of increasing receptor methylation. As the glutamyl residues within the adaptation domain become increasingly methylated the kinase control domain four-helix bundle becomes more tightly packed. However as the glutamyl residues are demethylated the kinase control domain four-helix bundle becomes loosely packed. If the kinase control domain four-helix bundle becomes too loosely packed or too tightly packed the kinase activity decreases. Therefore, there is an optimal packing of the kinase control domain four-helix bundle that allows for normal receptor function. The dotted lines on the curve represent the wild type Tar receptor kinase activity as a function of receptor methylation. The 0G/-4 mutant in a *cheR*$^+$*B*$^+$ strain (blue diamond) is overmethylated, CCW locked, and shows no aspartate chemotaxis. Whereas the 0G/-4 mutant in a *ΔcheRB* strain (red diamond) becomes less CCW biased. This suggests that the 0G/-4 mutant induces a conformation in HAMP that causes the adaptation domain to become overmethylated. This overmethylation, in turn could cause the kinase control domain four-helix bundle to pack too tight that it inhibits kinase activity. In the absence of the methylation machinery the lack of methylation results in the receptor retaining some kinase activation. The 2G mutant in a *cheR*$^+$*B*$^+$ strain (blue triangle) is demethylated, CCW biased, and is deficient in aspartate chemotaxis. However, the 2G mutant in a *ΔcheRB* strain (red triangle) is CCW locked. This suggests that in the absence of the methylation machinery, a distorted HAMP domain allows the kinase-control module to become too tightly packed in the QEQE state, resulting in a kinase inhibiting state and a CCW-locked phenotype. In the presence of CheB, however, deamidation/demethylation of the adaptation domain may loosen the packing of the kinase control module four-helix to create a kinase-activating conformation. The -2 mutant in a *cheR*$^+$*B*$^+$ strain (blue square) is demethylated, CCW biased, and is deficient in aspartate chemotaxis. However, the -2 mutant in a *ΔcheRB* strain resembles wild type rotational bias. This suggests that in this protein, the HAMP domain may be perturbed enough that the kinase-control module becomes slightly overwound in the QEQE state, resulting in a slightly higher CCW bias. In the presence of CheRB, the tighter packing of the kinase control module may evoke deamidation/demethylation of the receptor that causes an overcompensated loosening of the kinase-control module that leads to a further decrease in kinase stimulation.

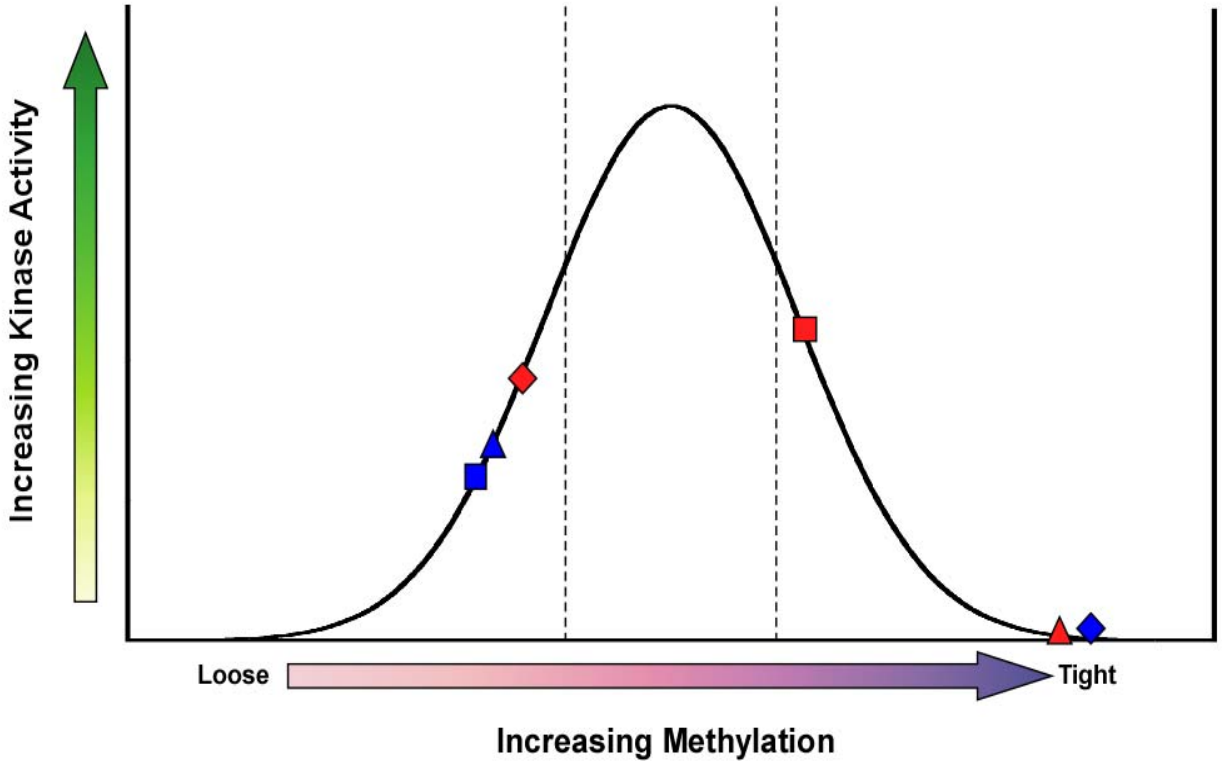
Increasing Kinase Activity
Loose
Tight
Increasing Methylation

Models for the mechanism of signaling from TM2 through HAMP to the kinase control module

As stated in Chapter I, there are two classes of models for how TM2 signals through HAMP to the kinase-control module. Briefly, one model for HAMP function suggests the AS1 and AS2 helices undergo a 26 degree rotation relative to each other upon the binding of attractant to the ligand-binding domain (*78*). An alternative model suggests that, in the absence of attractant, AS1 interacts with the cytoplasmic face of the membrane. Upon binding attractant, the AS1 domain is displaced from the membrane by the piston-like movement of TM2 (*73*).

The analyses of the TnG receptors and most of the Gly-replacement receptors argue against the idea that a rotational signal is transmitted directly from TM2 to HAMP. If the signal were rotational, then the insertion of flexible Gly residues between TM2 and HAMP should essentially eliminate the ability of TM2 to signal to HAMP, which is not the case. The results do not, however, eliminate the possibility that the conformational change within HAMP is a rotation of helices, but it is difficult to imagine how piston-like movement of TM2 results in helical rotation within HAMP.

The results from the TM2-HAMP junction Gly mutants are consistent with the membrane association model for HAMP function. The 4G receptor is very similar to wild-type Tar in every way except for its high level of methylation *in vivo* and the CCW-biased rotation of *cheR*$^{+}$*B*$^{+}$ cells producing the 4G receptor. Either shortening or lengthening the length of the Gly tether decreases, in a progressive, step-wise fashion, performance on aspartate semi-solid agar, suggesting that the 4-residue separation of

Tm2 from Pro-219 is critical. Shortening of the Gly connector does not lead to increased CW bias, which was the result seen when the distance between the aromatic WY tether and Pro-219 was decreased. Instead, in unstimulated cells kinase activity decreased, as though moving AS1 closer to the membrane prevents its proper alignment with regard to the membrane. However, the 2G receptor showed decreased methylation (or amidation) in its unstimulated state relative to the wild-type receptor, suggesting that the kinase-control domain may have been packed more tightly than in wild-type Tar.

In contrast, the experiments in which the MLLT putative helical connector was extended or shortened are not entirely consistent with the membrane-association model. Addition of residues decreases kinase-stimulating activity until the proper helical register is restored in the +3 and +4 receptors. In the simplest view of the membrane-association model, addition of residues in a helix should have the same effect as the addition of Gly residues. However, changing the helical register could interfere with the proper alignment of AS1 as well as the formation of the HAMP four-helix bundle, and the +3 and +4 mutants would come closest to restoring the original helical periodicity.

When the helical connection is shortened, the putative connector helix could be disrupted completely. It is noteworthy that removing only the Thr-218 residue does not disrupt receptor function very much, although it should cause a 100 degree axial rotation of AS1 if TM2 has a direct helical connection to AS1. However, the unstimulated -1 (MLL) receptor is overmethylated, whereas when the WY+1 receptor in the series in which the aromatic anchor were moved toward the periplasm the receptor is undermethylated. These two proteins should have the same number of residues between

the aromatic anchor and HAMP. The difference is that the helical register of the connector is not altered in the WY+1 receptor, whereas it is in the -1 (MLL) receptor.

The data presented here are completely consistent with the dynamic four-helix bundle model for regulation of the kinase control domain. However, although they eliminate a pure rotation model for transmembrane signaling, they do not unambiguously distinguish between the membrane-association and helical rotation models for HAMP function. To test the membrane-association model directly, I propose to use NBD fluorescence intensity and quenching experiments. The Tar protein has no native Cys residues, which makes it ideal for labeling with SH-reactive reagents. A previous study (*77*) demonstrated that every position in the Tar HAMP domain except Pro-219, Ile-230, Lys-237, and Ser-242 tolerates substitution with Cys. One can therefore substitute Cys at many positions within AS1 to label with the SH-reactive fluorescent probe NBD. NBD will be used because of its sensitivity to polar and nonpolar solvents. The individual cysteine substituted receptors will be overexpressed and enriched for in inner membrane vesicles (IMVs). The cys-substituted receptors within IMVs will be labeled with NBD and fluorescence measurements will be measured in the absence and presence of aspartate. If the NBD-labeled Cys is located in a nonpolar environment, such as the membrane of hydrophobic core of a protein, then the NBD fluorescence increases. However, if the NBD-labeled Cys residue is located in a polar environment, such as the cytosol, then the NBD fluorescence is decreased. A potential caveat to this experimentation is that NBD increases its fluorescence in a non-polar environment such as the hydrophobic interior of a protein or membrane. This

approach alone may not distinguish between residues interacting in the hydrophobic interior of the HAMP four-helix bundle and residues interacting with the hydrophobic core of the membrane.

To distinguish between a NBD-labeled Cys residues embedded in the membrane from a NBD-labeled Cys residue in the hydrophobic core of the HAMP four-helix bundle, nitroxide-labeled lipids can be used in the IMVs to quench the fluorescence of NBD-labeled cysteines that are embedded in the membrane. The IMVs which contain the mutant receptors that exhibited an increase in NBD fluorescence will be mixed with nitroxide-labeled phospholipids. The residues that show an increase in NBD fluorescence in the normal and a decrease in NBD fluorescence in the nitroxide-labeled IMVs should be embedded within the membrane. If the off state is the HAMP four-helix bundle then, when attractant is added, the residues that showed NBD fluorescence quenching should increase in NBD fluorescence.

REFERENCES

1. Berg, H. C., and Anderson, R. A. (1973) Bacteria swim by rotating their flagellar filaments, *Nature 245*, 380-382.

2. Berg, H. C., and Brown, D. A. (1972) Chemotaxis in *Escherichia coli* analysed by three-dimensional tracking, *Nature 239*, 500-504.

3. Silverman, M., and Simon, M. (1977) Chemotaxis in *Escherichia coli*: Methylation of che gene products, *Proc. Natl. Acad. Sci. U. S. A. 74*, 3317-3321.

4. Kondoh, H., Ball, C. B., and Adler, J. (1979) Identification of a methyl-accepting chemotaxis protein for the ribose and galactose chemoreceptors of *Escherichia coli*, *Proc. Natl. Acad. Sci. U. S. A. 76*, 260-264.

5. Hazelbauer, G. L., and Engstrom, P. (1980) Parallel pathways for transduction of chemotactic signals in *Escherichia coli*, *Nature 283*, 98-100.

6. Hazelbauer, G. L., Engstrom, P., and Harayama, S. (1981) Methyl-accepting chemotaxis protein III and transducer gene trg, *J. Bacteriol. 145*, 43-49.

7. Manson, M. D., Blank, V., Brade, G., and Higgins, C. F. (1986) Peptide chemotaxis in *E. coli* involves the Tap signal transducer and the dipeptide permease, *Nature 321*, 253-256.

8. Springer, M. S., Goy, M. F., and Adler, J. (1977) Sensory transduction in *Escherichia coli*: Two complementary pathways of information processing that involve methylated proteins, *Proc. Natl. Acad. Sci. U. S. A. 74*, 3312-3316.

9. Bibikov, S. I., Biran, R., Rudd, K. E., and Parkinson, J. S. (1997) A signal transducer for aerotaxis in *Escherichia coli*, *J. Bacteriol. 179*, 4075-4079.

10. Bibikov, S. I., Miller, A. C., Gosink, K. K., and Parkinson, J. S. (2004) Methylation-independent aerotaxis mediated by the *Escherichia coli* Aer protein, *J. Bacteriol. 186*, 3730-3737.

11. Rebbapragada, A., Johnson, M. S., Harding, G. P., Zuccarelli, A. J., Fletcher, H. M., Zhulin, I. B., and Taylor, B. L. (1997) The Aer protein and the serine chemoreceptor Tsr independently sense intracellular energy levels and transduce oxygen, redox, and energy signals for *Escherichia coli* behavior, *Proc. Natl. Acad. Sci. U. S. A. 94*, 10541-10546.

12. Reader, R. W., Tso, W. W., Springer, M. S., Goy, M. F., and Adler, J. (1979) Pleiotropic aspartate taxis and serine taxis mutants of *Escherichia coli*, *J. Gen. Microbiol. 111*, 363-374.

13. Krikos, A., Conley, M. P., Boyd, A., Berg, H. C., and Simon, M. I. (1985) Chimeric chemosensory transducers of *Escherichia coli*, *Proc. Natl. Acad. Sci. U. S. A. 82*, 1326-1330.

14. Milligan, D. L., and Koshland, D. E., Jr. (1988) Site-directed cross-linking. Establishing the dimeric structure of the aspartate receptor of bacterial chemotaxis, *J. Biol. Chem. 263*, 6268-6275.

15. Bowie, J. U., Pakula, A. A., and Simon, M. I. (1995) The three-dimensional structure of the aspartate receptor from *Escherichia coli*, *Acta. Crystallogr. D. Biol. Crystallogr. 51*, 145-154.

16. Milburn, M. V., Prive, G. G., Milligan, D. L., Scott, W. G., Yeh, J., Jancarik, J., Koshland, D. E., Jr., and Kim, S. H. (1991) Three-dimensional structures of the ligand-binding domain of the bacterial aspartate receptor with and without a ligand, *Science 254*, 1342-1347.

17. Scott, W. G., Milligan, D. L., Milburn, M. V., Prive, G. G., Yeh, J., Koshland, D. E., Jr., and Kim, S. H. (1993) Refined structures of the ligand-binding domain of the aspartate receptor from *Salmonella typhimurium*, *J. Mol. Biol. 232*, 555-573.

18. Russo, A. F., and Koshland, D. E., Jr. (1983) Separation of signal transduction and adaptation functions of the aspartate receptor in bacterial sensing, *Science 220*, 1016-1020.

19. Aravind, L., and Ponting, C. P. (1999) The cytoplasmic helical linker domain of receptor histidine kinase and methyl-accepting proteins is common to many prokaryotic signalling proteins, *FEMS Microbiol. Lett. 176*, 111-116.

20. Williams, S. B., and Stewart, V. (1999) Functional similarities among two-component sensors and methyl-accepting chemotaxis proteins suggest a role for linker region amphipathic helices in transmembrane signal transduction, *Mol. Microbiol. 33*, 1093-1102.

21. Krikos, A., Mutoh, N., Boyd, A., and Simon, M. I. (1983) Sensory transducers of *E. coli* are composed of discrete structural and functional domains, *Cell 33*, 615-622.

22. Kim, K. K., Yokota, H., and Kim, S. H. (1999) Four-helical-bundle structure of the cytoplasmic domain of a serine chemotaxis receptor, *Nature 400*, 787-792.

23. Liu, J. D., and Parkinson, J. S. (1991) Genetic evidence for interaction between the CheW and Tsr proteins during chemoreceptor signaling by *Escherichia coli*, *J. Bacteriol. 173*, 4941-4951.

24. Ames, P., Yu, Y. A., and Parkinson, J. S. (1996) Methylation segments are not required for chemotactic signalling by cytoplasmic fragments of Tsr, the methyl-accepting serine chemoreceptor of *Escherichia coli*, *Mol. Microbiol. 19*, 737-746.

25. Wu, J., Li, J., Li, G., Long, D. G., and Weis, R. M. (1996) The receptor binding site for the methyltransferase of bacterial chemotaxis is distinct from the sites of methylation, *Biochemistry 35*, 4984-4993.

26. Ames, P., Studdert, C. A., Reiser, R. H., and Parkinson, J. S. (2002) Collaborative signaling by mixed chemoreceptor teams in *Escherichia coli*, *Proc. Natl. Acad. Sci. U. S. A. 99*, 7060-7065.

27. Studdert, C. A., and Parkinson, J. S. (2004) Crosslinking snapshots of bacterial chemoreceptor squads, *Proc. Natl. Acad. Sci. U. S. A. 101*, 2117-2122.

28. Studdert, C. A., and Parkinson, J. S. (2005) Insights into the organization and dynamics of bacterial chemoreceptor clusters through in vivo crosslinking studies, *Proc Natl Acad Sci U S A 102*, 15623-15628.

29. Ames, P., and Parkinson, J. S. (2006) Conformational suppression of inter-receptor signaling defects, *Proc. Natl. Acad. Sci. U. S. A. 103*, 9292-9297.

30. McAndrew, R. S., Ellis, A. E., Manson, M. D., and Holzenburg, A. (2004) TEM analysis of chemoreceptor arrays of *E. coli* in native membranes, *Microsc. Microanal. 10*, 416-417.

31. McAndrew, R. S., Ellis, A. E., Lai, R. Z., Manson, M. D., and Holzenburg, A. (2005) Identification of Tsr and Tar chemoreceptor arrays in *E. coli* inner membranes, *Microsc. Microanal. 11*, 1190-1191.

32. Studdert, C. A., and Parkinson, J. S. (2005) Insights into the organization and dynamics of bacterial chemoreceptor clusters through in vivo crosslinking studies, *Proc. Natl. Acad. Sci. U. S. A. 102*, 15623-15628.

33. Maddock, J. R., and Shapiro, L. (1993) Polar location of the chemoreceptor complex in the *Escherichia coli* cell, *Science 259*, 1717-1723.

34. Sourjik, V., and Berg, H. C. (2000) Localization of components of the chemotaxis machinery of *Escherichia coli* using fluorescent protein fusions, *Mol Microbiol 37*, 740-751.

35. Shiomi, D., Zhulin, I. B., Homma, M., and Kawagishi, I. (2002) Dual recognition of the bacterial chemoreceptor by chemotaxis-specific domains of the CheR methyltransferase, *J Biol Chem 277*, 42325-42333.

36. Cantwell, B. J., Draheim, R. R., Weart, R. B., Nguyen, C., Stewart, R. C., and Manson, M. D. (2003) CheZ phosphatase localizes to chemoreceptor patches via CheA-short, *J Bacteriol 185*, 2354-2361.

37. Banno, S., Shiomi, D., Homma, M., and Kawagishi, I. (2004) Targeting of the chemotaxis methylesterase/deamidase CheB to the polar receptor-kinase cluster in an *Escherichia coli* cell, *Mol Microbiol 53*, 1051-1063.

38. Sourjik, V., and Berg, H. C. (2002) Receptor sensitivity in bacterial chemotaxis, *Proc Natl Acad Sci U S A 99*, 123-127.

39. Bourret, R. B., Hess, J. F., and Simon, M. I. (1990) Conserved aspartate residues and phosphorylation in signal transduction by the chemotaxis protein CheY, *Proc. Natl. Acad. Sci. U. S. A. 87*, 41-45.

40. Sockett, H., Yamaguchi, S., Kihara, M., Irikura, V. M., and Macnab, R. M. (1992) Molecular analysis of the flagellar switch protein FliM of *Salmonella typhimurium*, *J. Bacteriol. 174*, 793-806.

41. Welch, M., Oosawa, K., Aizawa, S., and Eisenbach, M. (1993) Phosphorylation-dependent binding of a signal molecule to the flagellar switch of bacteria, *Proc. Natl. Acad. Sci. U. S. A. 90*, 8787-8791.

42. Roman, S. J., Meyers, M., Volz, K., and Matsumura, P. (1992) A chemotactic signaling surface on CheY defined by suppressors of flagellar switch mutations, *J. Bacteriol. 174*, 6247-6255.

43. Shukla, D., Zhu, X. Y., and Matsumura, P. (1998) Flagellar motor-switch binding face of CheY and the biochemical basis of suppression by CheY mutants that compensate for motor-switch defects in *Escherichia coli*, *J. Biol. Chem. 273*, 23993-23999.

44. Sourjik, V., and Berg, H. C. (2002) Binding of the *Escherichia coli* response regulator CheY to its target measured in vivo by fluorescence resonance energy transfer, *Proc Natl Acad Sci U S A 99*, 12669-12674.

45. Barak, R., and Eisenbach, M. (1992) Correlation between phosphorylation of the chemotaxis protein CheY and its activity at the flagellar motor, *Biochemistry 31*, 1821-1826.

46. Alon, U., Camarena, L., Surette, M. G., Aguera y Arcas, B., Liu, Y., Leibler, S., and Stock, J. B. (1998) Response regulator output in bacterial chemotaxis, *Embo. J. 17*, 4238-4248.

47. Cluzel, P., Surette, M., and Leibler, S. (2000) An ultrasensitive bacterial motor revealed by monitoring signaling proteins in single cells, *Science 287*, 1652-1655.

48. Hess, J. F., Oosawa, K., Matsumura, P., and Simon, M. I. (1987) Protein phosphorylation is involved in bacterial chemotaxis, *Proc. Natl. Acad. Sci. U. S. A. 84*, 7609-7613.

49. Segall, J. E., Manson, M. D., and Berg, H. C. (1982) Signal processing times in bacterial chemotaxis, *Nature 296*, 855-857.

50. Springer, M. S., Goy, M. F., and Adler, J. (1979) Protein methylation in behavioural control mechanisms and in signal transduction, *Nature 280*, 279-284.

51. Brown, D. A., and Berg, H. C. (1974) Temporal stimulation of chemotaxis in Escherichia coli, *Proc. Natl. Acad. Sci. U. S. A. 71*, 1388-1392.

52. Terwilliger, T. C., Bogonez, E., Wang, E. A., and Koshland, D. E., Jr. (1983) Sites of methyl esterification on the aspartate receptor involved in bacterial chemotaxis, *J. Biol. Chem. 258*, 9608-9611.

53. Terwilliger, T. C., and Koshland, D. E., Jr. (1984) Sites of methyl esterification and deamination on the aspartate receptor involved in chemotaxis, *J. Biol. Chem. 259*, 7719-7725.

54. Kehry, M. R., Bond, M. W., Hunkapiller, M. W., and Dahlquist, F. W. (1983) Enzymatic deamidation of methyl-accepting chemotaxis proteins in *Escherichia coli* catalyzed by the cheB gene product, *Proc. Natl. Acad. Sci. U. S. A. 80*, 3599-3603.

55. Goy, M. F., Springer, M. S., and Adler, J. (1977) Sensory transduction in *Escherichia coli*: Role of a protein methylation reaction in sensory adaptation, *Proc. Natl. Acad. Sci. U. S. A. 74*, 4964-4968.

56. Springer, M. S., Goy, M. F., and Adler, J. (1977) Sensory transduction in *Escherichia coli*: A requirement for methionine in sensory adaptation, *Proc. Natl. Acad. Sci. U. S. A. 74*, 183-187.

57. Ames, P., and Parkinson, J. S. (1994) Constitutively signaling fragments of Tsr, the *Escherichia coli* serine chemoreceptor, *J Bacteriol 176*, 6340-6348.

58. Ames, P., Yu, Y. A., and Parkinson, J. S. (1996) Methylation segments are not required for chemotactic signalling by cytoplasmic fragments of Tsr, the methyl-accepting serine chemoreceptor of *Escherichia coli*, *Mol Microbiol 19*, 737-746.

59. Ames, P., and Parkinson, J. S. (2006) Conformational suppression of inter-receptor signaling defects, *Proc Natl Acad Sci U S A 103*, 9292-9297.

60. Boldog, T., Grimme, S., Li, M., Sligar, S. G., and Hazelbauer, G. L. (2006) Nanodiscs separate chemoreceptor oligomeric states and reveal their signaling properties, *Proc Natl Acad Sci U S A 103*, 11509-11514.

61. Biemann, H. P., and Koshland, D. E., Jr. (1994) Aspartate receptors of *Escherichia coli* and *Salmonella typhimurium* bind ligand with negative and half-of-the-sites cooperativity, *Biochemistry 33*, 629-634.

62. Yeh, J. I., Biemann, H. P., Prive, G. G., Pandit, J., Koshland, D. E., Jr., and Kim, S. H. (1996) High-resolution structures of the ligand binding domain of the wild-type bacterial aspartate receptor, *J Mol Biol 262*, 186-201.

63. Chi, Y. I., Yokota, H., and Kim, S. H. (1997) Apo structure of the ligand-binding domain of aspartate receptor from *Escherichia coli* and its comparison with ligand-bound or pseudoligand-bound structures, *FEBS Lett 414*, 327-332.

64. Hughson, A. G., and Hazelbauer, G. L. (1996) Detecting the conformational change of transmembrane signaling in a bacterial chemoreceptor by measuring effects on disulfide cross-linking in vivo, *Proc Natl Acad Sci U S A 93*, 11546-11551.

65. Ottemann, K. M., Xiao, W., Shin, Y. K., and Koshland, D. E., Jr. (1999) A piston model for transmembrane signaling of the aspartate receptor, *Science 285*, 1751-1754.

66. Chervitz, S. A., and Falke, J. J. (1995) Lock on/off disulfides identify the transmembrane signaling helix of the aspartate receptor, *J Biol Chem 270*, 24043-24053.

67. Lai, W. C., Peach, M. L., Lybrand, T. P., and Hazelbauer, G. L. (2006) Diagnostic cross-linking of paired cysteine pairs demonstrates homologous structures for two chemoreceptor domains with low sequence identity, *Protein Sci 15*, 94-101.

68. Draheim, R. R., Bormans, A. F., Lai, R. Z., and Manson, M. D. (2006) Tuning a bacterial chemoreceptor with protein-membrane interactions, *Biochemistry 45*, 14655-14664.

69. Trammell, M. A., and Falke, J. J. (1999) Identification of a site critical for kinase regulation on the central processing unit (CPU) helix of the aspartate receptor, *Biochemistry 38*, 329-336.

70. Starrett, D. J., and Falke, J. J. (2005) Adaptation mechanism of the aspartate receptor: electrostatics of the adaptation subdomain play a key role in modulating kinase activity, *Biochemistry 44*, 1550-1560.

71. Lai, R. Z., Bormans, A. F., Draheim, R. R., Wright, G. A., and Manson, M. D. (2008) The region preceding the C-terminal NWETF pentapeptide modulates baseline activity and aspartate inhibition of Escherichia coli Tar, *Biochemistry 47*, 13287-13295.

72. Aravind, L., and Ponting, C. P. (1999) The cytoplasmic helical linker domain of receptor histidine kinase and methyl-accepting proteins is common to many prokaryotic signalling proteins, *FEMS Microbiol Lett 176*, 111-116.

73. Williams, S. B., and Stewart, V. (1999) Functional similarities among two-component sensors and methyl-accepting chemotaxis proteins suggest a role for linker region amphipathic helices in transmembrane signal transduction, *Mol Microbiol 33*, 1093-1102.

74. Utsumi, R., Brissette, R. E., Rampersaud, A., Forst, S. A., Oosawa, K., and Inouye, M. (1989) Activation of bacterial porin gene expression by a chimeric signal transducer in response to aspartate., *Science 245*, 1246-1249.

75. Baumgartner, J. W., Kim, C., Brissette, R. E., Inouye, M., Park, C., and Hazelbauer, G. L. (1994) Transmembrane signalling by a hybrid protein: Communication from the domain of chemoreceptor Trg that recognizes sugar-binding proteins to the kinase/phosphatase domain of osmosensor EnvZ, *J Bacteriol 176*, 1157-1163.

76. Ward, S. M., Delgado, A., Gunsalus, R. P., and Manson, M. D. (2002) A NarX-Tar chimera mediates repellent chemotaxis to nitrate and nitrite, *Mol. Microbiol. 44*, 709-719.

77. Butler, S. L., and Falke, J. J. (1998) Cysteine and disulfide scanning reveals two amphiphilic helices in the linker region of the aspartate chemoreceptor, *Biochemistry 37*, 10746-10756.

78. Hulko, M., Berndt, F., Gruber, M., Linder, J. U., Truffault, V., Schultz, A., Martin, J., Schultz, J. E., Lupas, A. N., and Coles, M. (2006) The HAMP domain structure implies helix rotation in transmembrane signaling, *Cell 126*, 929-940.

79. Swain, K. E., and Falke, J. J. (2007) Structure of the conserved HAMP domain in an intact, membrane-bound chemoreceptor: a disulfide mapping study, *Biochemistry 46*, 13684-13695.

80. Ames, P., Zhou, Q., and Parkinson, J. S. (2008) Mutational analysis of the connector segment in the HAMP domain of Tsr, the *Escherichia coli* serine chemoreceptor, *J Bacteriol 190*, 6676-6685.

81. Watts, K. J., Ma, Q., Johnson, M. S., and Taylor, B. L. (2004) Interactions between the PAS and HAMP domains of the *Escherichia coli* aerotaxis receptor Aer, *J Bacteriol 186*, 7440-7449.

82. Watts, K. J., Sommer, K., Fry, S. L., Johnson, M. S., and Taylor, B. L. (2006) Function of the N-terminal cap of the PAS domain in signaling by the aerotaxis receptor Aer, *J Bacteriol 188*, 2154-2162.

83. Draheim, R. R., Bormans, A. F., Lai, R. Z., and Manson, M. D. (2005) Tryptophan Residues Flanking the Second Transmembrane Helix (TM2) Set the Signaling State of the Tar Chemoreceptor, *Biochemistry 44*, 1268-1277.

84. Danielson, M. A., Biemann, H. P., Koshland, D. E., Jr., and Falke, J. J. (1994) Attractant- and disulfide-induced conformational changes in the ligand binding domain of the chemotaxis aspartate receptor: A 19F NMR study, *Biochemistry 33*, 6100-6109.

85. Chervitz, S. A., Lin, C. M., and Falke, J. J. (1995) Transmembrane signaling by the aspartate receptor: Engineered disulfides reveal static regions of the subunit interface, *Biochemistry 34*, 9722-9733.

86. Chervitz, S. A., and Falke, J. J. (1996) Molecular mechanism of transmembrane signaling by the aspartate receptor: A model, *Proc Natl Acad Sci U S A 93*, 2545-2550.

87. Scott, W. G., and Stoddard, B. L. (1994) Transmembrane signalling and the aspartate receptor, *Structure 2*, 877-887.

88. Winston, S. E., Mehan, R., and Falke, J. J. (2005) Evidence that the adaptation region of the aspartate receptor is a dynamic four-helix bundle: Cysteine and disulfide scanning studies, *Biochemistry 44*, 12655-12666.

89. Berg, H. C., and Block, S. M. (1984) A miniature flow cell designed for rapid exchange of media under high-power microscope objectives, *J Gen Microbiol 130*, 2915-2920.

90. Bormans, A. F. (2005) *Intradimer and interdimer methylation response by bacterial chemoreceptors to attractant stimulus*, Ph.D. dissertation, Texas A&M University, College Station TX.

91. Shrout, A. L., Montefusco, D. J., and Weis, R. M. (2003) Template-directed assembly of receptor signaling complexes, *Biochemistry 42*, 13379-13385.

92. Levit, M. N., Liu, Y., and Stock, J. B. (1999) Mechanism of CheA protein kinase activation in receptor signaling complexes, *Biochemistry 38*, 6651-6658.

93. Kim, S. H. (1994) "Frozen" dynamic dimer model for transmembrane signaling in bacterial chemotaxis receptors, *Protein Sci 3*, 159-165.

VITA

Name:	Gus Alan Wright
Address:	Department of Biological Sciences, Vanderbilt University, U5215 MRB III, 465 21st Avenue South, Nashville, TN 37232
Email address:	gusalanwright@gmail.com
Education:	B.S., Cellular and Molecular Biology, University of Alabama at Birmingham, 2000 Ph.D., Biochemistry, Texas A&M University, 2009